Invasion and maintenance of spore killing in ascomycete fungi

Ivain Martinossi-Allibert[1], Carl Veller[2,3], S. Lorena Ament-Velásquez[1], Aaron A. Vogan[1], Claus Rueffler*[4], and Hanna Johannesson*[1]

[1]Department of Organismal Biology, Uppsala University, Sweden

[2]Department of Organismic and Evolutionary Biology, Harvard University, USA

[3]Program for Evolutionary Dynamics, Harvard University, USA

[4]Department of Ecology and Genetics, Animal Ecology, Uppsala University, Sweden

*Both authors contributed equally

September 2019

Abstract

Meiotic drivers are common selfish genetic elements that have the ability to become over-represented among the products of meiosis, a transmission advantage that allows them to spread in a population even when they impose fitness costs on their host organisms. The ability of a meiotic driver to invade a population, and to subsequently reach fixation or coexist in a stable polymorphism can be affected by features of the life-cycle, behavior, and population structure of their host organism. Here, we present a mathematical model that addresses several unexplored aspects of meiotic drive population genetics, by focusing on spore killing, a type of drive specific to fungi. Our model can be adapted to different fungal life-cycles, and is used here to specifically analyze the cases of two well-studied genera of filamentous ascomycetes known to harbor spore killing elements, *Podospora* and *Neurospora*. We show how ploidy level, rate of selfing, and efficiency of spore killing affect the invasion probability of a driving allele and conditions for its coexistence in a stable polymorphism. Our theoretical findings are discussed in light of recent empirical findings in these two systems.

1 Introduction

Our understanding of population genetics relies on the expectation that any two copies of a gene in a diploid genome are equally represented among the products of meiosis — this is Mendel's first law (Lyttle, 1993). However, some genetic elements are able to distort the meiotic process in such a way as to become over-represented in meiotic products, a phenomenon called 'meiotic drive' (Sandler and Novitski, 1957; Burt and Trivers, 2006). Because of their ability to distort meiosis, meiotic drivers (MDs) gain a selective advantage at the gene level that allows them to increase in frequency in a population even when they impose fitness costs on their host organism, which can lead to population extinction (Hamilton, 1967; Pinzone and Dyer, 2013; Akbari et al., 2013; Kyrou et al., 2018). This genetic conflict that arises between a MD and its host can affect many evolutionary processes (Rice, 2013). For example, rapid co-evolution between MDs and counteracting genes called suppressors can accelerate speciation by creating genetic incompatibilities between recently separated populations (Frank, 1991), as well as shape genetic architecture in other important ways (Henikoff et al., 2001; Hurst and Werren, 2001; Werren, 2011). MDs can also affect mating behavior, since their spread can be impeded by, for example, inbreeding (Hurst and Werren (2001); Bull et al. (2019)) and multiple mating (Haig and Bergstrom, 1995).

MDs were discovered as early as the 1940s (Rhoades, 1942) and have been studied extensively since then. Early empirical observations were closely followed by theoretical work aimed at understanding the unique behavior of these selfish genetic elements (see for example Hiraizumi, 1962; Lewontin and Dunn, 1960; Lewontin, 1968, on the *t-haplotype* in mice). Theoretical work has focused on two key aspects of meiotic drive dynamics: under what conditions can a MD (i) invade a population and (ii) coexist at a stable equilibrium with a non-driving allele? These questions have been investigated with reference to a wide variety of species known to harbor MDs (e.g. Lewontin and Dunn, 1960; Hall and Dawe, 2018; Fishman and Kelly, 2015; Charlesworth and Hartl, 1978; Brand et al., 2015), which has revealed some general patterns of MD dynamics. First, since MDs are over-represented among successful meiotic products, theory predicts that, in the absence of counteracting forces, they should increase in frequency and reach fixation. However, the presence of suppressor alleles or fitness costs associated with the MD can bring the invasion process to a halt, leading ultimately to either loss of the MD or prolonged coexistence with a non-driving allele. The presence of a strong recessive fitness cost to the MD appears as a typical condition for coexistence, allowing invasion of the MD but not fixation (e.g. Fishman and Kelly, 2015; Lewontin and Dunn, 1960; Holman et al., 2015). These general principles, however, are far from encompassing the complexity and diversity of MD dynamics. Indeed, although all MDs have in common

the ability to distort Mendelian proportions, the diversity of their modes of action as well as the details of the life cycle of each host make insights from one species often not applicable to others. In the present study, we develop a population genetics model of meiotic drive in ascomycete fungi, a widespread class of MDs that causes spore killing and for which invasion dynamics are under-studied. Our model sheds light on the specific dynamics of this particular type of drive with respect to the complex features of fungal life cycles and the unique mechanisms of drive of spore killers.

Mechanisms of drive can be classified into three types: female drive, male drive, and spore killing (reviewed in Burt and Trivers, 2006; Lindholm et al., 2016). Female drive, as observed in maize *Zea mays* (Buckler et al., 1999), the monkeyflower *Mimulus guttatus* (Fishman and Saunders, 2008), and the house mouse *Mus musculus* (Didion et al., 2015), takes advantage of the asymmetry of female meiosis by preferentially segregating the driving element to the egg. In contrast, in male drive, the MD acts by killing the meiotic products (male gametes) that carry a different allele [for example, the *t-haplotype* in *Mus musculus* and *domesticus* (Silver, 1985) and *SD* in *Drosophila melanogaster* (Larracuente and Presgraves, 2012)]. The mechanism of spore killing in fungi is similar to male drive in that meiotic products that do not carry the MD are killed, thus reducing the number of meiotic products in heterozygotes (Raju, 1994). Spore killer MDs were first described in *Podospora anserina* (Padieu and Bernet, 1967), and later in other species, including two within the genus *Neurospora* (Turner and Perkins, 1979), as well as in the fission yeast *Schizosaccharomyces pombe* (Zanders et al., 2014). The three types of drive mechanisms differ in the level of cost they impose on their host, as well as in the type of selective advantage obtained by the MD. In female drive, the MD replaces the alternative allele without suppressing meiotic products. As a consequence, female drive can impose little or no cost to its host, while the MD increases in absolute number of copies (i.e., it *replaces* the alternative allele). Such MDs have therefore been termed *absolute* drivers (Lyttle, 1991). Male drive and spore killing, however, result in only a relative increase of the MD because meiotic products carrying the alternative allele are killed and not replaced. Male drive and spore killing can therefore be referred to as *relative* drive (Lyttle, 1991). They impose a fitness cost to their host because the total number of meiotic products is reduced. This cost could be more important in spore killing because meiotic products of fungi are offspring (spores) and not gametes. It is important to note that the elimination of meiotic products in male drive may not always result in a purely relative type of drive. Indeed, because a large number of sperm cells have to compete to fertilize a small number of eggs, a reduction in sperm count does not immediately imply a reduction in male fertility (Hartl, 1972). Depending on the mating system considered, a male drive could then in theory be purely absolute

if females mate once and the reduction in sperm count does not affect male fertility, or purely relative if post-copulatory competition is so intense that male reproductive success is reduced proportionally to the rate of sperm killing.

A relevant factor to consider in male drive and spore killing is the possibility that the killing of some proportions of the meiotic products (gametes or spores) that do non carry the MD provides a fitness benefit to the surviving ones. In the remainder of the study, we refer to this fitness benefit as "killing advantage". In male drive, killing advantage is well known under the form of compensatory mechanisms in the host that evolve to minimize the cost to reproductive success resulting from the action of the MD. Such killing advantage of the compensation type can for example occur through the production of additional sperm to compensate for the loss caused by the sperm killing MD (as has been observed for example in the stalk-eyed fly *Teleopsis dalamanni*, Meade et al., 2019). It is interesting to note that although compensation mechanisms evolve as an adaptive response of the host, they also provide a killing advantage to the sperm killer as a side-effect by increasing the absolute number of sperm cells produced carrying the MD. Killing advantage can therefore contribute to making a male drive more of an absolute driver. In Box 1 we compare how purely relative male drive, male drive with killing advantage and female drive differ in terms of selective advantage and invasion dynamics. We see that purely relative male drive has a positively frequency-dependent selective advantage, which is minimal in the early invasion stages, when the MD is at low frequency (as previously pointed out by Nauta and Hoekstra, 1993). An absolute drive, female drive or male drive with killing advantage, on the other hand, has a higher initial selective advantage because it increases in absolute copy number when driving. This distinction suggests that it will be important to identify to which degree a spore killer acts as a relative or absolute drive in order to determine the selective advantage and consequently the population dynamics of the driver.

At a first glance, spore killing appears to be a purely relative drive. Contrary to male drive, in which case the MD is eliminating gametes with an unclear effect on the fitness of the host, fungi have predominantly haploid life-cycles. This means that the spore killer is directly eliminating some proportion of its host's offspring. This offspring killing means that the spore killer can only eliminate spores carrying the alternative allele but not replace them, being therefore unable to increase in absolute copy number. Nevertheless, several mechanisms may exist that could allow a spore killer to derive an absolute fitness advantage from killing. We propose that a direct killing advantage could arise under two scenarios. First, killing advantage could arise in the form of compensation, in a form similar to what is found in male drive, where, as spore killing occurs during spore development, it is possible for parental energy to be reallocated from the killed

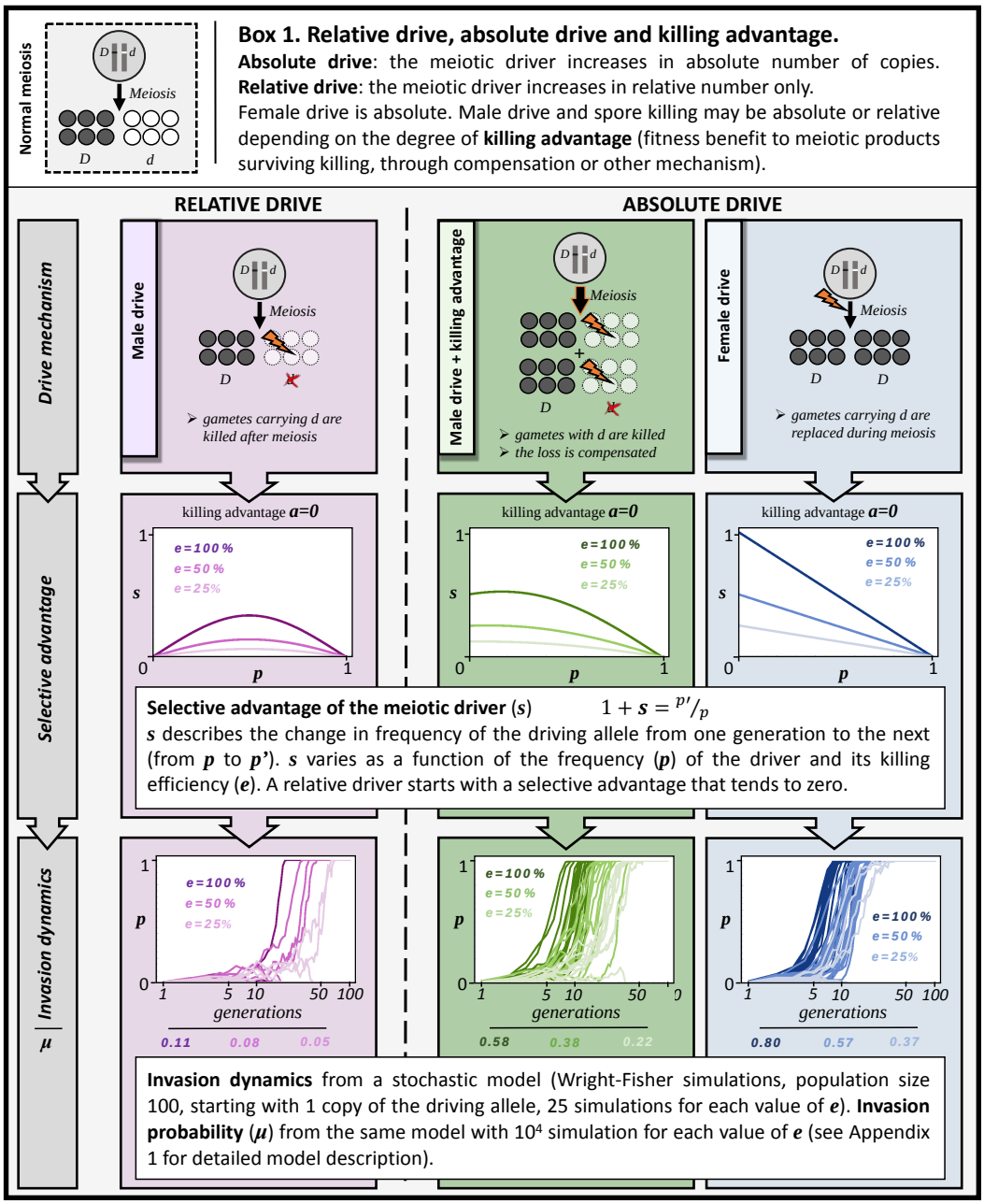

spores to either provide the surviving spores with extra resources or to produce additional spores. Second, a direct killing advantage could also take place if there is local resource competition among sibling spores. In this case, killing would provide surviving spores with a fitness advantage in the form of additional resources available for growth (Nauta and Hoekstra, 1993; Lindholm et al., 2016). In both scenarios, the killing advantage provides the spore killer with a fitness benefit that makes it more akin to an absolute drive mechanism.

In the present study, we develop a single-locus population genetics model of a spore killing MD in an ascomycete fungi host. Our model is based on the life cycle of *Podospora*, which has a

dikaryotic vegetative stage and reproduces by a combination of selfing and outcrossing. The model can be adapted to fungi with different life cycles such as fungi of the genus *Neurospora*, which have a haploid vegetative stage and reproduce sexually by obligate outcrossing between individuals of different mating types. For these two systems we analyse (i) the probability of invasion of a spore killing MD, and (ii) the conditions for the maintenance of a MD at intermediate frequencies in a population. Our model allows for arbitrary degrees of killing efficiency and killing advantage, as well as fitness costs imposed by the MD to its host at different stages of the life cycle. The effect of selfing rate and killing efficiency on the invasion and maintenance of the MD is also investigated. Throughout, we incorporate recent empirical findings to focus on relevant parameters.

We find that killing advantage is a crucial parameter to allow for the invasion of a spore killer MD, especially if drift is important. In the absence of selfing, incomplete killing and some level of fitness cost are necessary for a stable coexistence between the spore killer and the non-driving allele to be possible. When the selfing rate is higher however, coexistence is possible with fully efficient killing. As in other drive systems, a recessive fitness cost encourages coexistence, but we also find that killing advantage allows for coexistence even if the cost is not recessive. The space for coexistence also depends on the stage of the life-cycle at which the fitness cost of carrying a spore killer occurs. In light of empirical data, our model suggests that the observed spore killer frequencies in natural population of *Podospora* and *Neurospora* could be explained by a recessive cost of the spore killer combined with high selfing rates in *Podospora*. In addition, some degree of killing advantage should be expected as invasion appears unlikely in its complete absence.

2 The model

We study a diploid single-locus two-allele population genetics model in discrete time with non-overlapping generations. The two alleles are the spore killer D and the non-driving sensitive d. The life cycle characteristics we consider correspond to that of filamentous ascomycetes of the genera *Podospora* and *Neurospora*. Both of these taxa are model systems in fungal genetics and harbor spore killing elements (Silar, 2013; Vogan et al., 2019; Svedberg et al., 2020). Moreover, while the life cycle of *Podospora* has several lineage specific characteristics, the life cycle of *Neurospora* is representative of many other filamentous ascomycetes. Our model takes into account the rate of selfing (s), the killing efficiency of the allele D (e), the probability of first-division segregation at the spore killing locus during meiosis (f, see Figure 1), the costs of carrying the spore killer allele at different stages of the life cycle (z, k, k_m, g), and the possibility for a killing advantage (a) during spore killing events. For most of our analysis, we assume that the population is sufficiently

large that drift can be ignored. Under this assumption, we determine the parameter combinations that allow for the invasion of the spore killer allele D, and then ask whether invasion results in fixation of D, or whether the alleles D and d can coexist in a stable polymorphism. We then relax the assumption of infinitely large population size and explore the role of drift in the early phase of invasion of the spore killer allele by means of a Wright-Fisher model. Finally, in the discussion we contextualize our results with data from field and laboratory studies.

2.1 Life cycle and recursion equations

Figure 1 presents the life cycle of *Podospora*, which leads to a set of recursion equations describing the frequency dynamics of the spore killer allele D. The life cycle starts at the meiosis stage (left panel of Figure 1), which occurs in ascomycete fungi shortly after formation of the diploid zygote. Each diploid cell undergoes meiosis followed by one mitosis, resulting in the formation of a single ascus containing eight haploid nuclei. These nuclei can be packaged into pairs, forming a dikaryotic spore (two haploid nuclei in the same cytoplasm), or stay isolated, resulting in the formation of a monokaryotic spore (haploid). Monokaryons differ from dikaryons at the reproductive stage in that they cannot self.The probability that an ascus contains one monokaryon pair is denoted m. In *Podospora*, the frequency of monokaryotic spores is low (van der Gaag, 2005) and we assume that an ascus can never contain more than one pair of monokaryotic spores. Allele segregation during meiosis from heterozygote diploid cells can result in the formation of either heteroallelic or homoallelic dikaryotic spores. In case of first-division segregation at the spore killer locus, occurring with probability f, two homoallelic spores are formed. In the case of second-division segregation, occurring with probability $1-f$, four heteroallelic spores are formed. The left panel in Figure 1 represents all the possible outcomes of meiosis leading to the formation of different types of monokaryotic and dikaryotic spores. When monokaryotic spores of genotype d or dikaryotic spores of genotype dd share an ascus with spores of genotype D,DD or Dd, they are killed with probability e. Dikaryotic spores of the Dd genotype are not affected by spore killing. The frequency of each type of spore in the population after meiosis is denoted in the recursion equation by a capital letter M with a subscript indicating the genotype. For example the frequency of dikaryotic spores carrying two D alleles is denoted by M_{DD} and of monokaryotic spores of the d genotype by M_d. After meiosis, both dikaryotic and monokaryotic spores germinate and form a mycelium, which is the vegetative growth stage of the life cycle. We assume that monokaryons and dikaryons do not experience different growth rates during that vegetative stage. The vegetative stage is followed by the reproductive stage, which is represented in the right panel of Figure 1. Dikaryons

and monokaryons contribute to a common pool of randomly mating gametes, and dikaryons have the additional possibility of selfing (selfing probability s). Selfing in *Podospora* can only occur when a dikaryon carry nuclei of the two different mating types, and we assume here that selfing is always possible for a dikaryon because the mating-type locus always undergoes second-division segregation during meiosis, making all dikaryons automatically heteroallelic for the mating-type locus (in nature, the rate of second-division segregation of the mating-type locus is not 100% but very close). As a consequence of this mating type constraint, a heteroallelic dikaryon of genotype $D:d$ can only produce heterozygote diploid zygotes Dd through selfing.

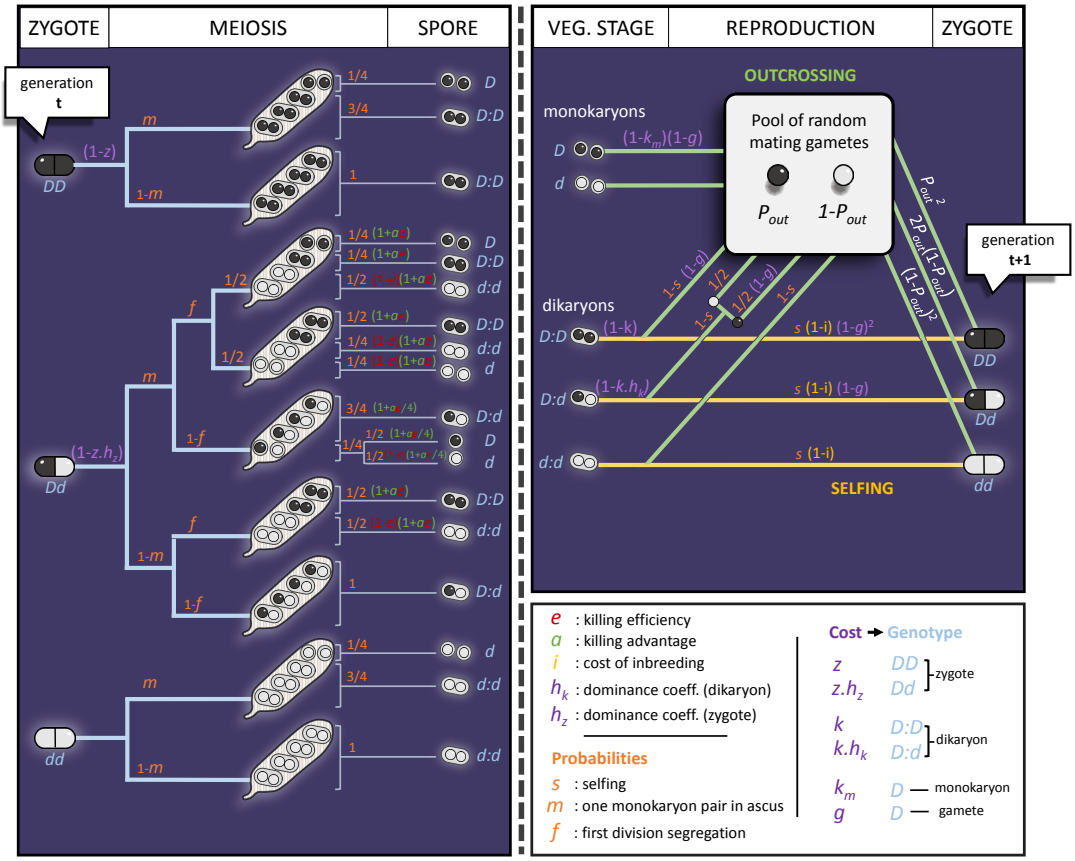

Figure 1: **Life cycle diagram of *Podospora*.** The life cycle is presented from zygote to zygote. The left panel represents the meiosis stage occurring shortly after zygote formation, and shows asci representing all possible segregation patterns of D and d from the three possible diploid genotypes. The right panel shows the reproductive stage with the outcrossing and selfing modes of reproduction, leading to fertilization and the formation of the diploid zygotes of the next generation. We update the frequencies of genotypes at each step of the life cycle given parameters as follow: purple symbols represent potential fitness costs associated with carrying the spore killer allele D, orange symbols represent probabilities of alternative events (for example, selfing occurring with probability s versus outcrossing occurring with probability $1-s$).Green symbols represent killing advantage (a) associated with spore killing events, while killing efficiency (e) is colored in red. Finally, the cost of inbreeding (i) at all loci associated with selfing is represented in yellow. The recursion equations can be constructed by following the lines of the life cycle diagram and multiplying each genotype frequency with the costs and probabilities that apply to it.

2.1.1 Structure of the recursions

Since we consider a population that can reproduce through both selfing and outcrossing, we cannot assume overall random mating. As a consequence, we need three recursions to follow the frequencies of the diploid genotypes DD, Dd and dd. Each generation, some individuals from each genotype are produced through selfing and some through outcrossing. Thus, the change in frequency for the three genotypes DD, Dd and dd is given by

$$p'_{DD} = \Big[selfing_{DD}(p_{DD}, p_{Dd}, p_{dd}) + outcrossing_{DD}(p_{DD}, p_{Dd}, p_{dd})\Big]\frac{1}{\bar{W}} \tag{1a}$$

$$p'_{Dd} = \Big[selfing_{Dd}(p_{DD}, p_{Dd}, p_{dd}) + outcrossing_{Dd}(p_{DD}, p_{Dd}, p_{dd})\Big]\frac{1}{\bar{W}} \tag{1b}$$

$$p'_{dd} = \Big[selfing_{dd}(p_{DD}, p_{Dd}, p_{dd}) + outcrossing_{dd}(p_{DD}, p_{Dd}, p_{dd})\Big]\frac{1}{\bar{W}}, \tag{1c}$$

where the frequency at the next time step is indicated by a dash and $\bar{W}$ represents mean fitness. We introduce the full expressions for how selfing and outcrossing contribute to the different genotype frequencies in the next section.

2.1.2 Detailed recursions

We first describe the contributions of the two possible modes of reproduction, selfing and outcrossing, to the diploid genotype frequencies of the next generation. The treatment of selfing and outcrossing is inspired by a plant population genetics model with self fertilization (Holsinger et al., 1984). Starting with the selfing part, with the support of the right hand panel from Figure 1, we can see that we need to take into account the frequencies of the three possible dikaryotic genotypes after meiosis, M_{DD}, M_{Dd} and M_{dd}. Dikaryons carrying the spore killing allele may pay a fitness cost in the homoallelic $(1-k)$ or heteroallelic form $(1-kh_k)$, with h_k being the dominance coefficient of the dikaryotic fitness cost. Genotype frequencies are then adjusted by the selfing probability s, and all genotypes are exposed to a potential cost of selfing $(1-i)$ due to inbreeding. Finally, because gametes are produced during the selfing process, individuals carrying the spore killer genotype are exposed to paying a gametic cost during selfing, ($(1-g)^2$ and $1-g$ respectively for dikaryons of the $D:D$ and $D:d$ genotypes). We can now write the selfing contribution to next generation's diploid genotype frequencies as a function of dikaryotic genotype frequencies after meiosis as

$$selfing_{DD} = M_{DD}(1-k)s(1-i)(1-g)^2 \tag{2a}$$

$$selfing_{Dd} = M_{Dd}(1-kh_k)s(1-i)(1-g) \tag{2b}$$

$$selfing_{dd} = M_{dd}s(1-i) \tag{2c}$$

Next, the outcrossing part of the life cycle is built assuming random mating. We call p_{out} the frequency of the spore killing allele D in the pool of random mating gametes. It is important to note that p_{out} only represents a valid frequency within the outcrossing fraction of the total population, which is denoted T_{out}. We can write the outcrossing contributions to the genotype frequencies of next generation as Hardy-Weinberg frequencies weighted by the fraction represented by the outcrossing population, so as to represent valid frequencies in the total population.

$$outcrossing_{DD} = T_{\text{out}} \times p_{\text{out}}^2 \tag{3a}$$

$$outcrossing_{Dd} = T_{\text{out}} \times 2p_{\text{out}}(1-p_{\text{out}}) \tag{3b}$$

$$outcrossing_{dd} = T_{\text{out}} \times (1-p_{\text{out}})^2 \tag{3c}$$

Now that we have described the contributions of selfing and outcrossing to the diploid genotype frequencies of generation $t+1$, we need to explicitly define T_{out}, p_{out}, $\bar{W}$ and all the genotype frequencies after meiosis M_{DD}, M_{Dd}, M_{dd}, M_D and M_d as functions of the diploid genotype frequencies at time t to complete the recursions.

T_{out} represents the outcrossing fraction of the population, in the form of a pool of random mating gametes. To this pool of gametes contribute all monokaryotic individuals (with potential fitness cost $(1-k_m)$ for monokaryons carrying the D allele) together with the fraction of dikaryons that engage in outcrossing with probability $(1-s)$. p_{out} represents the sub-part of the pool of random mating gametes carrying the D allele.

$$\begin{aligned} T_{\text{out}} = {} & M_D(1-k_m)(1-g) + M_d \\ & + (1-s)\Big(M_{DD}(1-k)(1-g) + M_{Dd}(1-kh_k)(1-\frac{g}{2}) + M_{dd}\Big) \end{aligned} \tag{4a}$$

$$\begin{aligned} p_{\text{out}} = {} & \Big(M_D(1-k_m)(1-g) \\ & + (1-s)\left(M_{DD}(1-k)(1-g) + M_{Dd}(1-kh_k)\frac{(1-g)}{2}\right)\Big)\frac{1}{T_{\text{out}}} \end{aligned} \tag{4b}$$

Following the meiosis diagram from the left hand panel of Figure 1, we can then define the genotype frequencies after meiosis taking into account the probability for an ascus to contain monokaryons m, the probability of first-division segregation f, killing efficiency e, and killing advantage a. When monokaryons are formed, they represent 1/4 of the nuclei in an ascus, and such asci occur with probability m. Consequently monokaryotic spores represent a fraction $m/4$ of the starting diploid frequencies, and dikaryons a fraction $(\frac{3}{4}m + (1-m))$. The starting frequencies of diploid genotypes are also exposed to associated diploid cost, $(1-z)$ for DD and $(1-zh_z)$ for Dd, with h_z being the dominance coefficient of the diploid cost. Then, spore killing is integrated in the recursions with the factor $(1-e)$, which affects monokaryotic spores of the d genotype and dikaryotic spores of the dd genotype that originate from Dd diploids. Importantly, the monokaryotic spores d are affected in both cases of first and second-division segregation, while dikaryotic spores are affected only if homoallelic (dd), and therefore only in case of first-division segregation (probability f). If killing efficiency $e = 1$, all the spores exposed to spore killing are suppressed. Finally, in asci where spore killing occurs, all surviving spores can benefit from the killing advantage regardless of their genotype. The killing advantage is assumed to originate from additional resources made available by spore killing, it is therefore proportional to the number of spores killed. For this reason, killing advantage is weighted by killing efficiency, providing a benefit $1 + ae$ to surviving spores. Killing advantage is also reduced in the case of second-division segregation of an ascus containing monokaryotic spores, since in that case only one nucleus per ascus is killed in contrast to the four killed nuclei of a first-division segregation killing. When this occurs, the killing advantage is $1 + \frac{ae}{4}$.

$$M_D = \frac{m}{4}\left(p_{DD}(1-z) + p_{Dd}(1-zh_z)\left(\frac{f}{2}(1+ae) + (1-f)\frac{(1+\frac{ae}{4})}{2}\right)\right) \tag{5a}$$

$$M_d = \frac{m}{4}\left(p_{dd} + (1-e)p_{Dd}(1-zh_z)\left(\frac{f}{2}(1+ae) + (1-f)\frac{(1+\frac{ae}{4})}{2}\right)\right) \tag{5b}$$

$$M_{DD} = \left(\frac{3}{4}m + (1-m)\right)\left(p_{DD}(1-z) + p_{Dd}(1-zh_z)\frac{f}{2}(1+ae)\right) \tag{5c}$$

$$M_{Dd} = \left(\frac{3}{4}m + (1-m)\right)p_{Dd}(1-zh_z)(1-f)\left(1+\frac{ae}{4}\right) \tag{5d}$$

$$M_{dd} = \left(\frac{3}{4}m + (1-m)\right)\left(p_{dd} + (1-e)p_{Dd}(1-zh_z)\frac{f}{2}(1+ae)\right) \tag{5e}$$

Finally, $\bar{W}$ is the sum of the numerators of p'_{DD}, p'_{Dd} and p'_{dd} as defined in equation 1.

2.2 The model adapted to *Podospora*

The model described above is a adapted to the life cycle of *Podospora*. In this section we define limits on parameter ranges that can be determined from knowledge of the biological system. It is unknown in this system whether spore killing alleles impose a fitness cost to the carrier. Therefore, we study the broadest possible range of fitness costs for each stage of the life cycle, from 0 (no cost) to 1 (fully lethal). Similarly, whether killing advantage occurs in *Podospora* and to which extent is currently unknown, so we explore a wide range of killing advantage from 0 (no benefit) to 1 (equivalent to all killed spores being replaced). The rate of selfing in natural population is also not known, but the propensity of *Podospora* species to self in laboratory conditions, together with low overall levels of genetic diversity (Vogan et al., 2019), indicate that it may be high. We study the effect of several rates of selfing on spore killer dynamics, from 0 to 95%. Spore killer alleles known in *Podospora* exhibit probabilities of first-division segregation that range from about 30% to 100% (van der Gaag et al., 2000; Vogan et al., 2019), we therefore broadly cover this range by studying 25%,50% and 100% probability of first-division segregation. In natural condition, the occurrence of asci containing monokaryons can vary between 0% and 6% (Esser, 1974; van der Gaag, 2005). We therefore analyse the model without monokaryons first, and then with a probability of occurrence of 1% and 5% to cover the natural range of occurrence, and 50% to make the effect on spore killing dynamics more visible. Finally, killing efficiency (e), i.e. the propensity to kill when the killer and sensitive alleles are packaged in the same ascus, is considered to be high in *Podospora*. For the main part, the model is analyzed with $e = 1$ but we also explore briefly the effect of incomplete killing ($e < 1$) in order to contrast its effect with incomplete first-division segregation ($f < 1$). This last part is also useful in drawing a parallel between the *Podospora* model and the *Neurospora* model, where incomplete killing plays a more important role.

2.3 The model adapted to *Neurospora*

We focus on the life cycles of heterothallic *Neurospora* species such as *N. sitophila* and *N. crassa*, which can be modelled with simplifications of the recursions for the *Podospora* life cycle. First and foremost, as these species are sexually self incompatible the entire population is outcrossing. We choose to assume here that reproduction occurs through random mating, although we acknowledge that inbreeding is a possibility in *Neurospora*. This assumption greatly simplifies the model as we do not need to track frequencies of diploid genotypes anymore. The model becomes one-dimensional (*versus* two-dimensional for *Podospora*) and the entire system can be described

by following the change of frequency of the allele D in the haploid stage. Additionally, the *Neurospora* species we are interested in have a dominantly haploid life cycle, with haploid spores and vegetative stage. This feature of the life cycle means that we do not need to model dikaryons and monokaryons, and that the rate of first-division segregation is unimportant to the action of the spore killer. In terms of parameters, these changes are implemented by fixing: $s = 0$, $m = 0$, $f = 1$. The recursion that describes the change in frequency of D can be written by starting from the frequency of D in the pool of random mating gametes and using Hardy-Weinberg frequencies for random fusion of gametes. The same diploid and haploid costs z and g as in the *Podospora* model apply, as well as killing efficiency e and killing advantage a.

Let p_D be the frequency of D in the gamete pool at generation t and p'_D at generation $t+1$. In that case,

$$p'_D = \frac{p_D^2 L_{DD} + p_D(1-p_D)L_D}{p_D^2 L_{DD} + 2p_D(1-p_D)(\frac{L_D}{2} + \frac{L_d}{2}) + (1-p_D)^2}, \tag{6}$$

where

$$L_{DD} = (1-z)(1-g) \tag{7a}$$

$$L_D = (1-zh_z)(1+ae)(1-g) \tag{7b}$$

$$L_d = (1-e)(1-zh_z)(1+ae) \tag{7c}$$

The notations of (7) are useful to make equation (6) more compact and readable, but they also carry biological meaning. L_{DD} represents the overall fitness cost associated with starting the life cycle as a DD zygote, L_D as a D nucleus in a Dd zygote and L_d a d nucleus in a Dd zygote, including the cost of being suppressed by spore killing.

2.4 Methods for analysing the recursions

We first analyse the recursions in a deterministic framework, with the aim of determining parameter ranges for which invasion, and subsequent fixation or stable polymorphism of the spore killing allele are possible. The general method we use to analyse the deterministic models is to identify equilibrium points of the system and determine their stability. The stability of equilibria is determined by linearizing the recursions around the equilibrium points and determining (i) the derivative of the recursion in the case of a one-dimensional system (*Neurospora*) (see pp. 163-172 Otto and Day, 2011) or (ii) the dominant eigenvalue of the resulting Jacobian matrices in the two-dimensional case (*Podospora*) (see pp. 316-320 Otto and Day, 2011).

In order to take into account drift due to finite population size, we then analyse a stochastic version of the model to determine the invasion probability of the spore killer. To do this, we implement the recursions into Wright-Fisher models, which introduces random sampling at the stage of zygote formation each generation. For a specific set of parameter values, the invasion probability is estimated as the proportion of 10^3 Wright-Fisher simulations in which the spore killer achieves its deterministic equilibrium frequency (fixation or stable polymorphism). If the deterministic equilibrium is instead loss of the spore killer, then the invasion probability is taken to be zero.

3 Results

3.1 Deterministic model

3.1.1 *Podospora*

In *Podospora* selfing can occur between dikaryotic individuals. Because of this non-random mating we must follow the frequency of diploid genotypes. We therefore use the full system of recursions from equation 1. In this case, we are unable to find general solutions for equilibrium frequencies and their stability. Instead, we can solve for equilibria when parameter values are set and we resort to parameter sweeps. At first, we assume that killing efficiency e is fixed to one, and that the rate of monokaryons m is zero, in order to study the effects of selfing, killing advantage, rate of first-division segregation and fitness costs to the spore killer. Later, we relax these assumptions and study the effects of e and m.

In figure 2 we present equilibrium values and stability for the case of a diploid recessive fitness cost of carrying the spore killer allele. We can see that there is a large space for stable polymorphism of the spore killer, requiring some degree of recessive fitness cost and of compensation. A recessive cost allows the spore killer to invade but prevents fixation (recessivity is important, as the cost will then only be substantial when the spore killer has already reached high frequencies). At the same time, with this cost being present, invasion is only possible if killing advantage is sufficient to give a net fitness benefit to spore killing. From figure 2, we can also see that the rate of first-division segregation f, which determines the frequency of spore killing in heterozygotes, and selfing rate s interact, with f favoring the fixation of the spore killer and s preventing its invasion. The largest space for polymorphism of the spore killer is found in the case where selfing rate and rate of first-division segregation are both low. Interestingly, these two parameters interact, with the effect of f on the dynamic of the spore killer being most obvious when selfing is absent

($s = 0$), and f having absolutely no effect when selfing rate is high. The reason for this is that killing efficiency only matters as long as the population of heterozygotes is not a limiting factor, since spore killing happens only in heterozygote individuals. Because new heterozygotes can only be produced through outcrossing and not selfing, a high selfing rate becomes the limiting factor for the rate of killing itself. A comparison with the results from the *Neurospora* model of the previous section clarifies the distinction between rate of first-division segregation, f and killing efficiency e. This distinction only arises if killing advantage is present, because in that case spores of the sensitive genotype surviving incomplete killing ($e < 1$) will benefit from the killing advantage as well, whereas spores surviving killing because of second-division segregation during meiosis ($f < 1$) will not. The main consequence of this distinction is that incomplete killing ($e < 1$) allows a stable polymorphism of the spore killer and the sensitive, even in the case of a non-recessive fitness cost to the killer, while second-division segregation ($f < 1$) only allows for a polymorphism in the case of a recessive fitness cost to the killer. This can be visualized with supplementary figures S2, S3, S4 and S5, were the additive and dominant case for both diploid (z) and dikaryotic (k) costs are shown, as well as haploid cost (g) in supplementary figure S6 and no parameter space allowing for a stable polymorphism can be observed. If we relax the assumption that $e = 1$ in *Podospora* however, we then see a parameter space appear that allows for a polymorphism in the case of an additive cost, even when the probability of first-division segregation is one (supplementary figures S7 and S8). This can be paralleled with the case of *Neurospora*, where the killing advantage gained by surviving non-driving spores in case of incomplete killing allows for a coexistence even if the fitness cost to the drive is not recessive. The dynamic is very similar to the case of *Neurospora* and we refer the reader to that section for a more detailed description of the phenomenon.

The stage of the life cycle at which the cost of carrying the spore killer is expressed is also crucial for the dynamics of the spore killer: in the case of a recessive dikaryotic fitness cost, the parameter space allowing for a stable polymorphism is somewhat reduced compared to the case of the recessive diploid cost (compare figure 2 and 3). This difference can be understood by looking back at the schematic of the life cycle in figure (1). In the case of a recessive diploid cost, heterozygote individuals in which spore killing occurs do not pay a fitness cost, which makes the spore killing event beneficial for the spore killing allele. However, in the case of a dikaryotic cost, spore killing occurs only in the event of first-division segregation (probability f), which leads to the production of homoallelic individuals that do pay the cost even if recessive. In other words, when the cost intervenes at the diploid stage, the spore killer can kill without paying the recessive cost, but if the cost intervenes at the dikaryotic stage, the spore killer can *either* kill *or* avoid the cost.

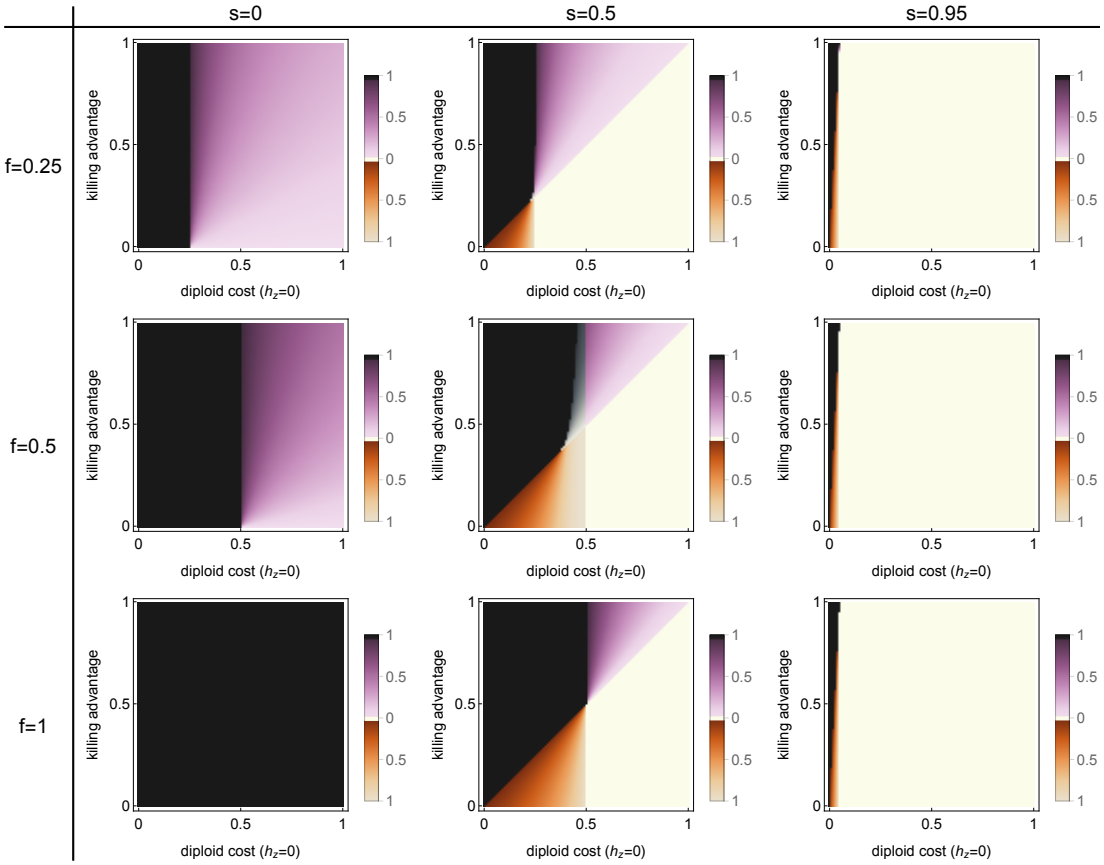

Figure 2: **Recessive Diploid cost ($h_z = 0$). Equilibrium values and stability of the spore killer in *Podospora*, as a function of fitness cost, selfing rate (s), rate of first-division segregation (f) and killing advantage.** Equilibrium value and stability were determined by solving the equation system that defines the model for Podospora. Each graph gives equilibrium values for 100 values of fitness cost and 100 values of killing advantage. White cells correspond to $p_D = 0$ being a stable equilibrium and $p_D = 1$ being the only other (unstable) equilibrium. In these cases the spore killer cannot invade. Black cells correspond to $p_D = 1$ being a stable equilibrium with $p_D = 0$ being the only other (unstable) equilibrium, which means that the spore killer can invade and goes to fixation. Shades of purple indicate a stable internal equilibrium, which value is indicated by the scale next to each plot, with both $p_D = 0$ and $p_D = 1$ unstable. In that case, the spore killer can invade but will not reach fixation, a stable polymorphism can exist. Finally, shades of brown represent an unstable internal equilibrium, with the value of the equilibrium frequency indicated by the shade of brown on the scale besides each plot. In that case, both $p_D = 0$ and $p_D = 1$ are stable, meaning that the spore killer shouldn't be able to invade, but if present in the population at a frequency higher than the unstable equilibrium, it can then reach fixation. The grey area represents a space where two internal equilibria exist, one stable and one unstable, with the shading intensity representing the value of the stable one. The unstable equilibrium is always higher than the stable one so this area represents a parameter space where invasion is possible.

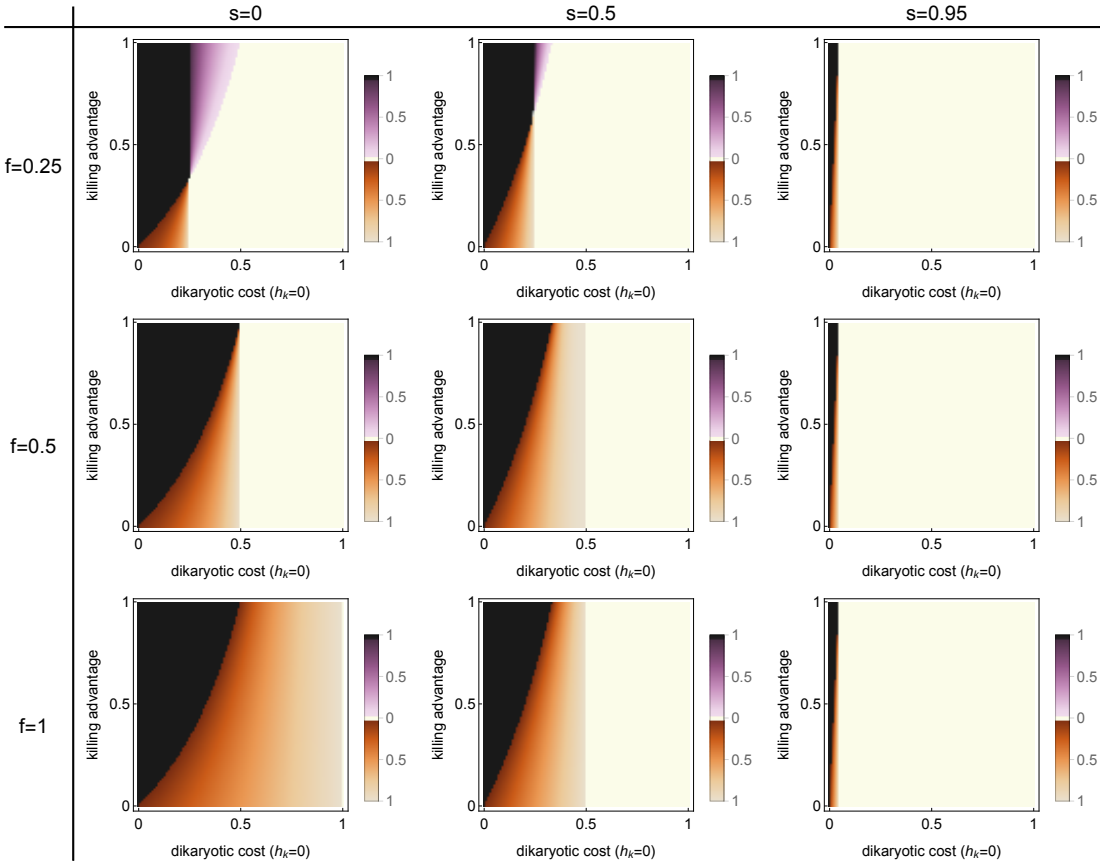

Figure 3: **Recessive Dikaryotic cost ($h_k = 0$). Equilibrium values and stability of the spore killer in *Podospora*, as a function of fitness cost, selfing rate (s), rate of first-division segregation (f) and killing advantage.** Equilibrium value and stability were determined by solving the equation system that defines the model for Podospora. Each graph gives equilibrium values for 100 values of fitness cost and 100 values of compensation. White cells correspond to $p_D = 0$ being a stable equilibrium and $p_D = 1$ being the only other (unstable) equilibrium. In these cases the spore killer cannot invade. Black cells correspond to $p_D = 1$ being a stable equilibrium with $p_D = 0$ being the only other (unstable) equilibrium, which means that the spore killer can invade and goes to fixation. Shades of purple indicate a stable internal equilibrium, which value is indicated by the shade on the scale next to each plot, with both $p_D = 0$ and $p_D = 1$ unstable. In that case, the spore killer can invade but will not reach fixation, a stable polymorphism can exist. Finally, shades of brown represent an unstable internal equilibrium, with the value of the equilibrium frequency indicated by the shade of brown on the scale besides each plot. In that case, both $p_D = 0$ and $p_D = 1$ are stable, meaning that the spore killer shouldn't be able to invade, but if present in the population at a frequency higher than the unstable equilibrium (for example due to migration), it can then reach fixation.

Finally, we will have a look at the effect that monokaryons may have on the dynamics of the spore killer. Going back to the recursions, we can expect monokaryons to have two effects: (i) to allow for a small amount of spore killing in case of second-division segregation and (ii) to reduce the effective selfing rate of the population as monokaryons can only outcross. If we extract from the main recursions an expression of killing rate:

$$K = P_{Dd}e(1 - h_z z)\left(\frac{f}{2} + \frac{m}{4}\frac{(1-f)}{2}\right) \tag{8}$$

We can see that, if first-division segregation probability is lower than one, killing rate becomes an increasing function of the proportion of asci containing monokaryons (m). The lower f is, the more important the effect of m on killing rate, however killing rate is always more efficiently increased by f than by m. It is important to note that when spore killing occurs in an ascus that contains a pair of monokaryons after second-division segregation, only the one sensitive spore with a single nucleus dies. As a consequence, monokaryons combined with second-division segregation should be equivalent to incomplete killing ($e < 1$) and can be expected to share some of the effects of incomplete killing on spore killing dynamics. Then, because monokaryons cannot self, increasing the proportion of asci containing monokaryons reduces the effective selfing rate of the population. This should also increase killing rate by producing more heterozygote individuals (see equation 8). This means that monokaryons could in theory be important for the dynamics of spore killing but this is unlikely at the rates found in natural populations (ranging from 0% to 5.8% depending on the individuals, van der Gaag, 2005). In Supplementary figures S9,S10 and S11, we show how monokaryons can affect the dynamics of spore killing with the case of a recessive diploid fitness cost, with first 1%, 5% and then 50% of asci containing a pair of monokaryons. 1%-5% covers the range expected in natural conditions, while 50% is shown to magnify the effect and make it more appreciable. These figures can be compared to main Figure 2 which shows the same dynamics (diploid recessive cost) without monokaryons. On the figure with 50% occurrence of monokaryons, we can see some of the expected effects. The effect of selfing rate on spore killing is not as pronounced as in the case without monokaryons, because monokaryons cannot self, thereby reducing the effective selfing rate of the population. In addition, the conditions for fixation of the spore killer are affected in a way similar to the effect of incomplete killing (compare to supplementary figure S7), suggesting that a high frequency of monokaryons could contribute to a space for coexistence between the spore killer and a non-driving allele.

In summary, a spore killer in *Podospora* will invade if it bears no fitness cost, or if the cost is out-weighted by the fitness benefit of killing advantage. The cost can be magnified if selfing occurs,

as selfing slows down the spread of the spore killer while the fitness cost is still expressed. Selfing also affects drive strength, interacting with the rate of first-division segregation to determine the effective killing rate. Coexistence between the spore killer and a non-driving allele is possible with different configurations: (i) if killing efficiency is 100% there needs to be a recessive fitness cost and either some amount of selfing or of second-division segregation during meiosis to allow for coexistence. (ii) if killing efficiency is lower than 100%, coexistence is possible even if the fitness cost to the drive is not recessive, but this requires high killing advantage. Finally, the presence of monokaryons can reduce the effective selfing rate and create similar dynamics to incomplete killing by allowing coexistence even if the fitness cost to the spore killer is not recessive.

3.1.2 *Neurospora*

Equation (6) allows to analytically determine equilibrium values and assess the conditions for their stability. An equilibrium $\hat{p_D}$ exists when $p'_D = p_D$. The solutions of

$$\hat{p_D} = \frac{\hat{p_D}^2 L_{DD} + \hat{p_D}(1-\hat{p_D})L_D}{\hat{p_D}^2 L_{DD} + 2\hat{p_D}(1-\hat{p_D})(\frac{L_D}{2} + \frac{L_d}{2}) + (1-\hat{p_D})^2} \tag{9}$$

will then give us all the possible equilibrium values for the system.

Factoring $\hat{p_D}$ out of the right hand side shows that $\hat{p_{D_1}} = 0$ is an equilibrium

$$\hat{p_D} = \hat{p_D}\frac{\hat{p_D} L_{DD} + (1-\hat{p_D})L_D}{\hat{p_D}^2 L_{DD} + 2\hat{p_D}(1-\hat{p_D})(\frac{L_D}{2} + \frac{L_d}{2}) + (1-\hat{p_D})^2}. \tag{10}$$

Next, simplifying by $\hat{p_D}$ and factoring $p_D - 1$ out shows that $\hat{p_{D_2}} = 1$ is also an equilibrium

$$(\hat{p_D} - 1)(\hat{p_D}(L_{DD} - (L_D + L_d) + 1) + L_D - 1) = 0. \tag{11}$$

That $\hat{p_{D_1}} = 0$ and $\hat{p_{D_2}} = 1$ are equilibria in that system comes as no surprise, as they represent the case where the allele D is either absent and therefore cannot invade, or is fixed and therefore cannot disappear. It will be interesting however to determine the conditions for stability of these two equilibria, as they determine the possibility for the spore killer to invade and go to fixation. Finally, we are left with solving:

$$\hat{p_D}(L_{DD} - (L_D + L_d) + 1) + L_D - 1 = 0$$

which should give us one final equilibrium. We note that if $L_D = 1$ and $(L_{DD} - (L_D + L_d) + 1 = 0$, then all values of p_D are equilibria but this is a very special case where the homozygote diploid

cost of carrying the spore killer is exactly equal to the cost suffered by the non driving allele during killing, and the cost to the killer is also completely recessive. This situation with exactly balancing costs is not very likely to arise in a biological system and for this reason in the rest of this section we will consider that these conditions are not met. We now have to solve for the last equilibrium value. We find that

$$p_{\hat{D}_3} = \frac{1 - L_D}{1 - (L_D + L_d) + L_{DD}}. \tag{12}$$

This last equilibrium is only biologically relevant if comprised between zero and one as it should represent a frequency. It would then indicate the possibility for an equilibrium at intermediate frequency of the driver allele D. We need to distinguish two cases depending on the sign of $1 - \boldsymbol{L_D}$.

case 1: $L_D > 1$. Biologically, $L_D > 1$ means that the killing advantage (weighted by the killing efficiency) is stronger than the cost of carrying the D allele in the Dd branch of the life cycle. In other words, the driver allele gets a net fitness benefit from driving. To have a polymorphism in that case, we need $p_{\hat{D}_3}$ to be comprised between zero and one

$$\begin{cases} p_{\hat{D}_3} & > & 0 \\ p_{\hat{D}_3} & < & 1, \end{cases}$$

equivalent to

$$\begin{cases} L_{DD} - (L_D + L_d) + 1 & < & 0 \\ L_{DD} - (L_D + L_d) + 1 & < & 1 - L_D. \end{cases}$$

The two inequalities can be summarized by

$$L_d > L_{DD}.$$

The biological meaning of that last condition is that the fitness cost to the D allele in the homozygote form should be higher that the cost payed by the d allele through both killing and shared cost in heterozygote form (remember that the "loads" L are factors, meaning that a smaller L implies a higher cost). We now have two conditions that make a polymorphism possible: $L_D > 1$, meaning that the D allele gets a net fitness benefit from driving and $L_d > L_{DD}$, which means that the D allele in homozygote form has lower fitness than d. The stability of that internal equilibria can be determined by evaluating $\frac{\mathrm{d}p'_D}{\mathrm{d}p_D}$, using equation (6), at each equilibrium value. Because we

know that there are exactly three equilibria, with $p_{\hat{D}_1} < p_{\hat{D}_3} < p_{\hat{D}_2}$, we can simply determine the stability of $p_{\hat{D}_1} = 0$ and deduce the stability of the other two. Evaluated at $p_D = 0$, $\frac{\mathrm{d}p'_D}{\mathrm{d}p_D} = L_D$. We are in the case where $L_D > 1$, which means that $\hat{P_{D_1}}$ is unstable. As a consequence, the internal equilibrium $p_{\hat{D}_3}$ must be stable, and the last equilibrium $\hat{P_{D_2}}$ unstable. In biological terms, this means that when these conditions are met, the spore killer can invade ($\hat{P_{D_1}}$ is unstable) but it will not go to fixation ($\hat{P_{D_2}}$ is unstable), instead it will reach a stable intermediate frequency $\hat{P_{D_3}}$.

In conclusion, a stable polymorphism is possible if the two conditions $L_D > 1$ and $L_d > L_{DD}$ are met. Going back to (7), we can see how these conditions relate to the original parameters. Broadly, $L_D > 1$ means that killing advantage a should be high enough to compensate for various possible fitness costs associated with the D allele when D is in a heteroallelic individual. This allows the D allele to invade the population (i.e. $p_{\hat{D}_1} = 0$ is unstable). $L_d > L_{DD}$ indicates that the D allele in homozygote form pays a fitness cost that is high enough to prevent it from reaching fixation (i.e. $p_{\hat{D}_2} = 1$ is unstable). It is important to note however that this last condition can only be met if the killing efficiency e is smaller than 1. If $e = 1$, then either D invades and goes to fixation or it doesn't invade, but there is no stable polymorphism possible. Figure 4 provides a graphical representation of the two conditions necessary for a stable polymorphism of the spore killer in *Neurospora* and shows how these conditions are affected by e, a, diploid cost z and the degree of dominance of the cost. It is immediately clear from the figure that (i) some degree of cost and killing advantage are necessary to allow for a stable polymorphism (ii) the more recessive the cost, the larger the parameter space allowing for coexistence. It is worth highlighting here a dynamic that is specific to spore killing and relies on the mechanism of killing advantage. Because killing advantage arises in the form of additional resources to spores surviving a spore killing event, it will also benefit non-carrier spores that would have survived killing if $e < 1$. This mechanism creates a space for coexistence of the killer with the non-driving allele that does not require the fitness cost to the spore killer to be recessive (see for example Figure 4, second column, where the cost is purely additive). This is made possible by what we may call a "recessive benefit" to the non-driving allele, which acts in a symmetrical way to the recessive cost to the killer in allowing for stable coexistence. Where the recessive cost creates a space for coexistence because it allows invasion but prevents fixation of the spore killer, the "recessive benefit" prevents fixation of the spore killer by providing a fitness advantage to the non-driving allele in the heterozygote form. This occurs because the non-driving allele benefits from killing advantage (again, only if killing is incomplete, $e < 1$) during spore killing events. Under certain parameter combinations, this advantage is enough to prevent fixation of the spore killer. In Figure 4, we demonstrate this effect

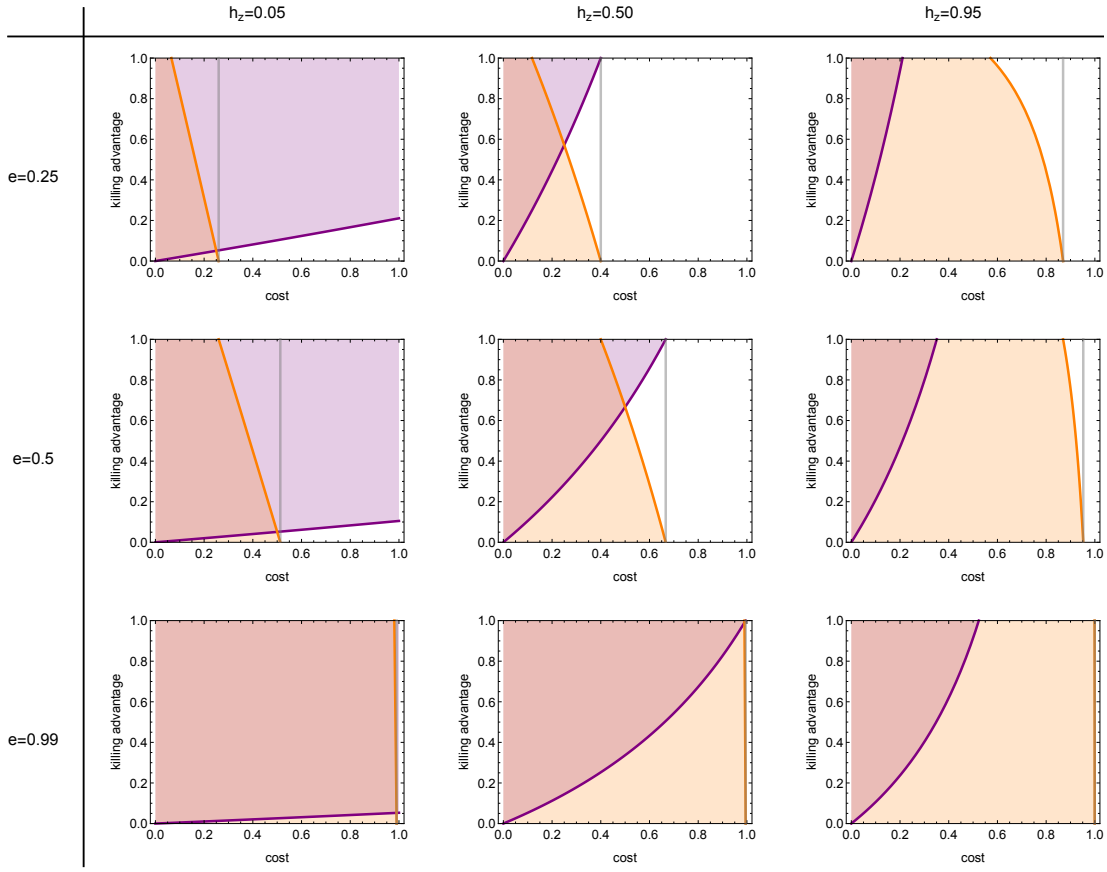

Figure 4: **Diploid fitness cost: parameter space allowing stable polymorphism of the spore killer in *Neurospora*.** Each graph is given for a different combination of killing efficiency of the spore killer (e) and degree of dominance (h_z) of the fitness cost of carrying that allele at the diploid stage. The intensity of the cost is represented on the x-axis of each graph and the degree of killing advantage (a) on the y-axis. The area above the purple line represents the parameter space where the spore killer can invade a population, starting from a frequency close to zero (corresponding to condition $L_D > 1$). To the left of the orange line is the parameter space where the spore killer can go to fixation when close to a frequency of one (corresponding to condition $L_d > L_{DD}$). A stable polymorphism is possible when the spore killer can invade (above the purple line) but not go to fixation (on the right of the orange line). The white area represents the parameter space where the spore killer is simply unable to invade or fix. The red-shaded area represents the parameter space where the spore killer can invade and goes to fixation. Finally, the yellow-shaded space represents a parameter space where the spore killer could go to fixation if starting from intermediate frequencies, but is unable invade. We make the assumption that non-driving spores that survive spore killing can also benefit from killing advantage. If we remove that assumption the orange line shifts to the grey line. We can see that in that new situation, the cost to the spore killer needs to be recessive for a stable polymorphism to be possible.

by showing the conditions for fixation of the spore killer in both cases where the non-driving allele is allowed to benefit from the killing advantage (orange line) or not (grey line). First, we can see that if $e = 1$, the grey and orange line overlap so that it does not matter if the non-driving allele benefits from killing advantage. Then, in cases where $e < 1$, we can see that the benefit to the non-driving allele makes an important change to the condition for fixation of the spore killer, making fixation of the killer more difficult as killing advantage increases. Similar dynamics apply

in the case of a haploid cost, with the difference that the cost is always expressed fully, there is no dominance parameter (See Supplementary Figure S1).

case 2: $L_D < 1$. In this case, $\hat{p_{D_1}} = 0$ is a stable equilibrium and the driver allele D is unlikely to invade. If an internal equilibrium exists, it is unstable and therefore does not represent the possibility for a stable polymorphism. If the internal equilibrium exist however, $\hat{p_{D_2}} = 1$ is stable, which means that if the allele D reaches a frequency higher than the unstable internal equilibrium (for example through migration from another population), it can go to fixation.

In summary, in the case of *Neurospora*, invasion of the spore killer is possible if there are no fitness costs, or if killing advantage outweighs fitness costs in heterozygote individuals. In addition, in the case where the killing advantage outweighs fitness costs, a stable coexistence is possible with the non-driving allele, provided that (i) killing is incomplete and (ii) there is either a strong fitness cost to the homozygote spore killer (recessive fitness cost) or a strong killing advantage to surviving spores that benefits surviving sensitive spores as well as killers (only possible if killing is incomplete).

3.2 Invasion probability

We estimate invasion probability for the *Podospora* and *Neurospora* models by implementing the recursions into a Wright-Fisher model. Invasion probability for a given set of parameter values is the proportion of 10^3 stochastic simulations for which the spore killing allele D reaches fixation or a stable internal equilibrium rather than becoming extinct.

3.2.1 *Podospora*

In *Podospora*, we find that whenever invasion is allowed by the deterministic model it can result in establishment of the spore killer, with a probability that depends on the strength of the drive (modulated by probability of first-division segregation), and the balance of fitness benefit (killing advantage) and costs (fitness cost weighted by selfing rate) associated to the spore killer. The degree of recessivity of the fitness cost is also an important parameter in affecting invasion probability. As stochastic extinction are likely to happen at low frequency, a stage where a purely recessive cost is expressed very little, it will not affect invasion probability to any large extent. Importantly, we find that when the spore killer is associated with killing advantage or fitness cost or both, the dependency of invasion probability on population size becomes negligible. We refer the reader to Box 2 earlier in this section for our analysis of the dependency of invasion probability on population size in the case where killing advantage and fitness cost are absent. In Figure 5

Box 2. Invasion probability of a simple spore killer.

Here, we consider the invasion probability of a simple spore killer without killing advantage. It is known that the selective advantage of such spore killers and consequently their invasion probability tends to zero as the population size N becomes large (Nauta and Hoekstra 1993). However, it has not been demonstrated how rapidly this invasion probability declines as N grows, and how the effects of population size on invasion probability and mutational supply interact to determine the rate of invasion of spore killers.

Invasion probability as a function of population size N.

We study the simplest possible model of a newly-arisen spore killer with 100% killing efficiency, assuming random mating (including no selfing). Employing a heuristic method from Desai and Fisher (2007, p.1763), we show in **Appendix 1** that, once the spore killer exceeds $n = \sqrt{N}$ copies, the expected increase in its copy number over the subsequent n generations ($\sim n^3/N$) is greater than typical decreases in copy number by random drift over the same period ($\sim n$), so that the spore killer has very likely escaped stochastic loss. The dynamics of the spore killer before reaching $\sqrt{N}$ copies are dominated by random drift, so the probability that it attains the required $\sqrt{N}$ copies — i.e., its invasion probability — is approximately: $\sqrt{N}/N = \mathbf{1}/\sqrt{\boldsymbol{N}}$. This approximation accords well with estimates obtained from simulations (see panel (a)).

Invasion rate as a function of population size N.

If spore killers arise at a rate μ per replication, then their rate of appearance per generation is $N\mu$. Therefore, the per-generation rate of invasion of such spore killers is $N\mu \times 1/\sqrt{N} = \sqrt{\boldsymbol{N}}\boldsymbol{\mu}$. The invasion rate is therefore an increasing function of population size (see panel (b)), despite the fact that the invasion probability of each individual spore killer is lower, and indeed tends to zero in the large-population limit. Additional life-history features, such as selfing, will affect invasion rate but will not affect the positive scaling with population size (panel (b)).

Invasion probability and population structure.

The dependence of the invasion probability on N suggests that population structure could significantly affect the rate at which spore killers invade. Suppose that the population of size N is subdivided into M demes, each of size $m = N/M$. The overall arrival rate of new spore killers is unchanged ($N\mu$) but, since invasion of one deme guarantees population-wide invasion (unless m is very small), the invasion probability is $1/\sqrt{m}$. The invasion rate is therefore $N\mu \times 1/\sqrt{m} = \mu\sqrt{m}\sqrt{N}$, larger than in an unstructured population by a factor $\sqrt{\boldsymbol{M}}$. A similar result has been obtained for recessive beneficial mutations, which are under similar frequency-dependent selection (Gale 1990, p.180-181).

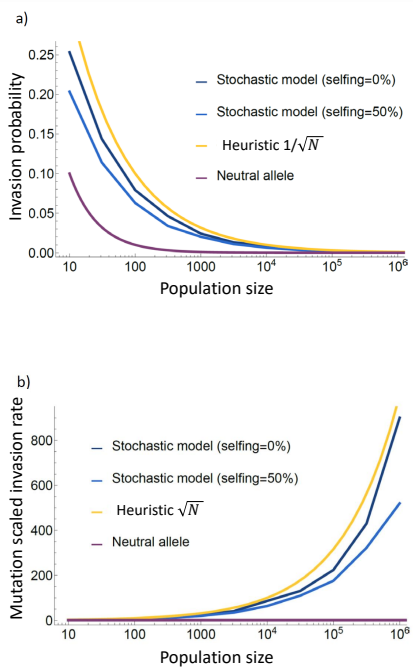

Take-home

Even spore killers without killing advantage can exhibit appreciably large invasion probability. They are expected to invade at a non-negligible rate, especially in large, fragmented populations, unless their appearance by mutation is extremely infrequent.

and 6 we show invasion probability for the *Podospora* model in the cases of recessive and additive diploid fitness costs. Other costs were also analyzed and can be found in Supplementary figures S12, S13, S14, S15.

3.2.2 Invasion probability in *Neurospora*

Similar to the case of *Podospora*, whenever invasion is allowed by the deterministic model it will happen with a probability that depends on drive strength (killing efficiency) and associated fitness cost and killing advantage. In Figure 8 and Figure 7, we show invasion probability for both the

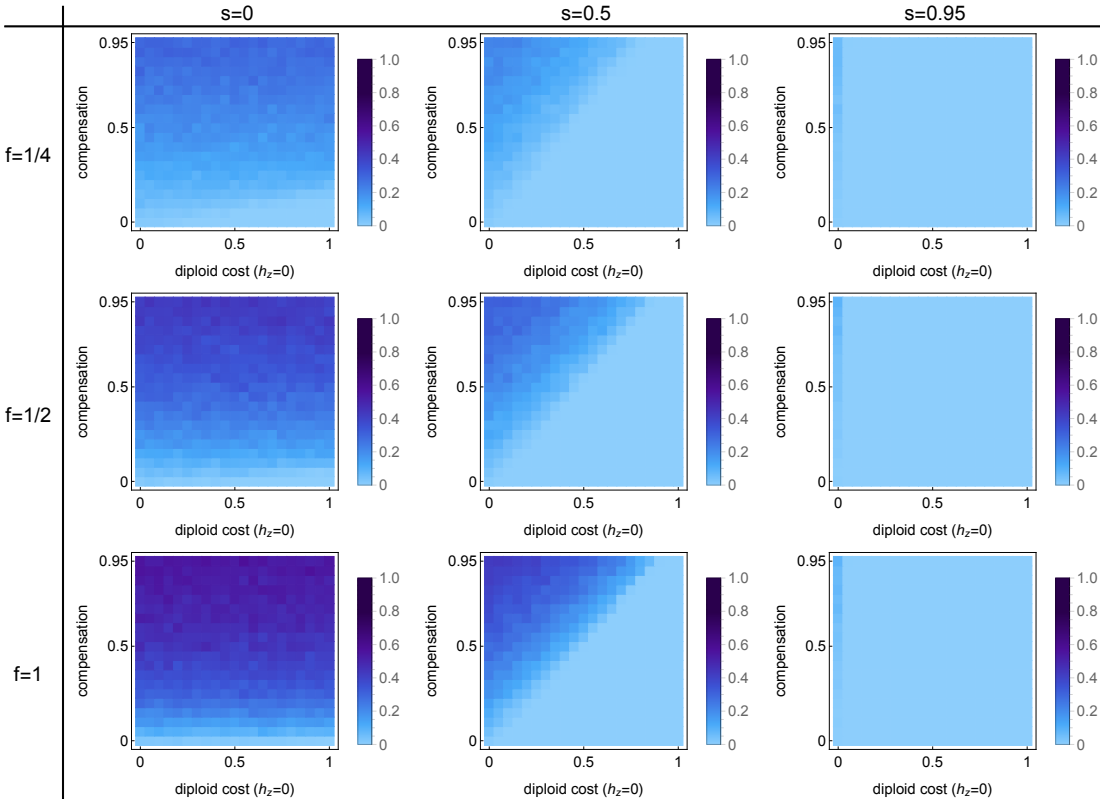

Figure 5: **Invasion probability of a spore killer with recessive diploid fitness cost ($h_z = 0$) in *Podospora* as a function of selfing rate (s), probability of first-division segregation (f) and killing advantage.** Each heatmap presents invasion probability of a spore killer allele as a function of fitness cost of carrying the allele (x-axis) and killing advantage a (y-axis). For each pixel, invasion probability is estimated from 10^3 stochastic simulations. Heatmaps are given for three values of selfing rate and three values of first-division segregation probability. The population size is 1000.

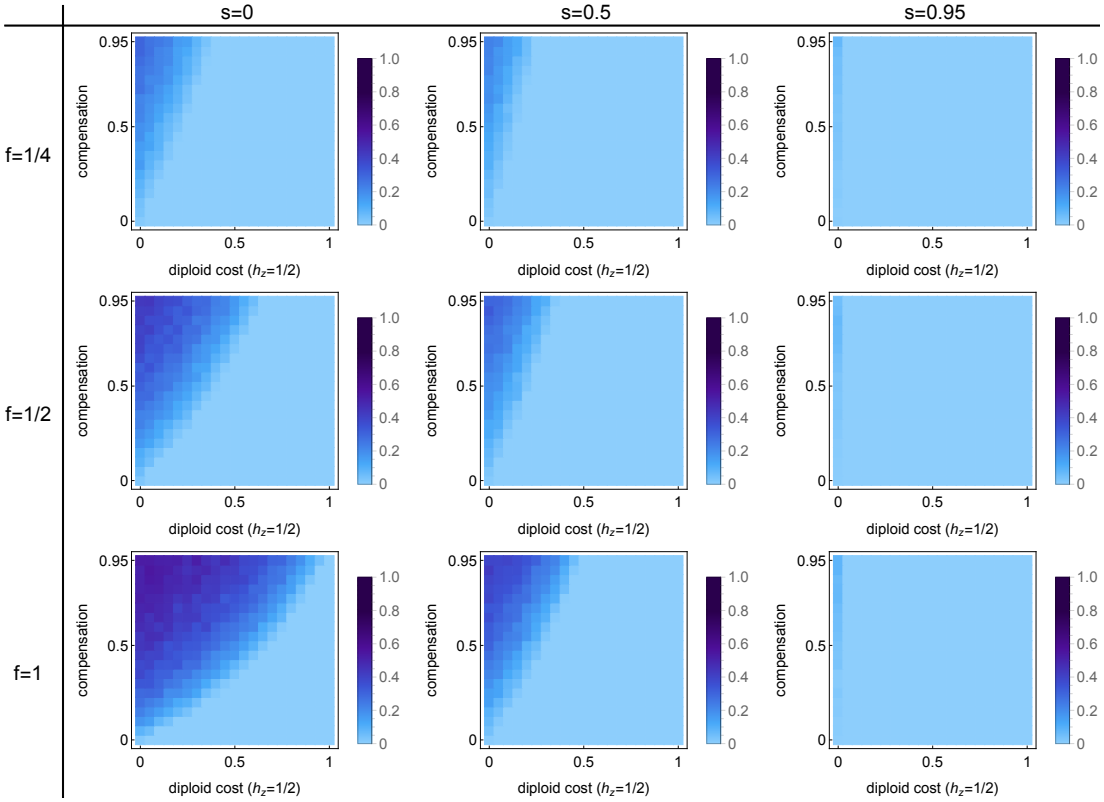

Figure 6: **Invasion probability of a spore killer with additive diploid fitness cost ($h_z = 1/2$) in *Podospora* as a function of selfing rate (s), probability of first-division segregation (f) and killing advantage.** Each heatmap presents invasion probability of a spore killer allele as a function of fitness cost of carrying the allele (x-axis) and killing advantage a (y-axis). For each pixel, invasion probability is estimated from 10^3 stochastic simulations. Heatmaps are given for three values of selfing rate and three values of first-division segregation probability. The population size is 1000.

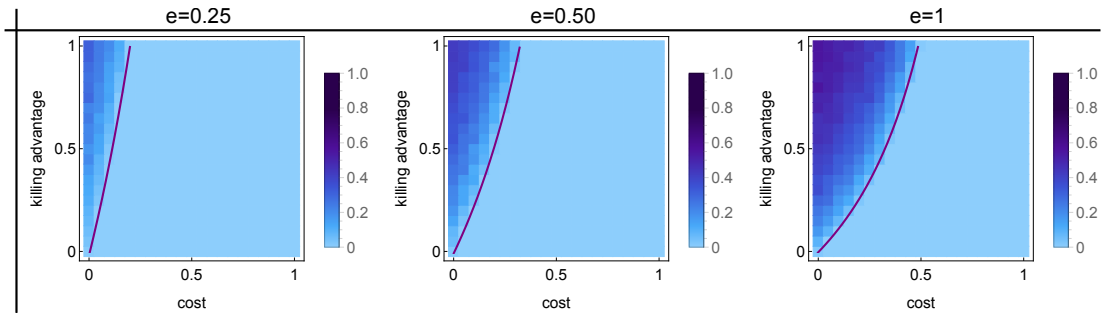

Figure 7: **Invasion probability of a spore killer with haploid fitness cost in *Neurospora* as a function of killing advantage.** Each heatmap presents invasion probability of a spore killer allele as a function of fitness cost of carrying the allele (x-axis) and killing advantage a (y-axis). For each pixel, invasion probability is estimated from 10^3 stochastic simulations. The population size is 1000. Heatmaps are given for three values of killing efficiency e. The purple line delineates the region of the parameter space that allows for invasion of the spore killer according to the deterministic analysis of the model (purple line from Supplementary figure S1), with invasion possible on the left side of the line.

cases of a diploid and haploid fitness cost to the spore killer. In the case of *Neurospora*, we can delineate the parameter space where invasion is allowed by the deterministic model, which we show on the figures with a red line. Similar to the case of *Podospora*, when the diploid fitness cost is recessive it has very little influence on invasion probability as the cost is not expressed early on in the invasion phase when stochastic extinctions are most likely to occur (Figure 8, left column).

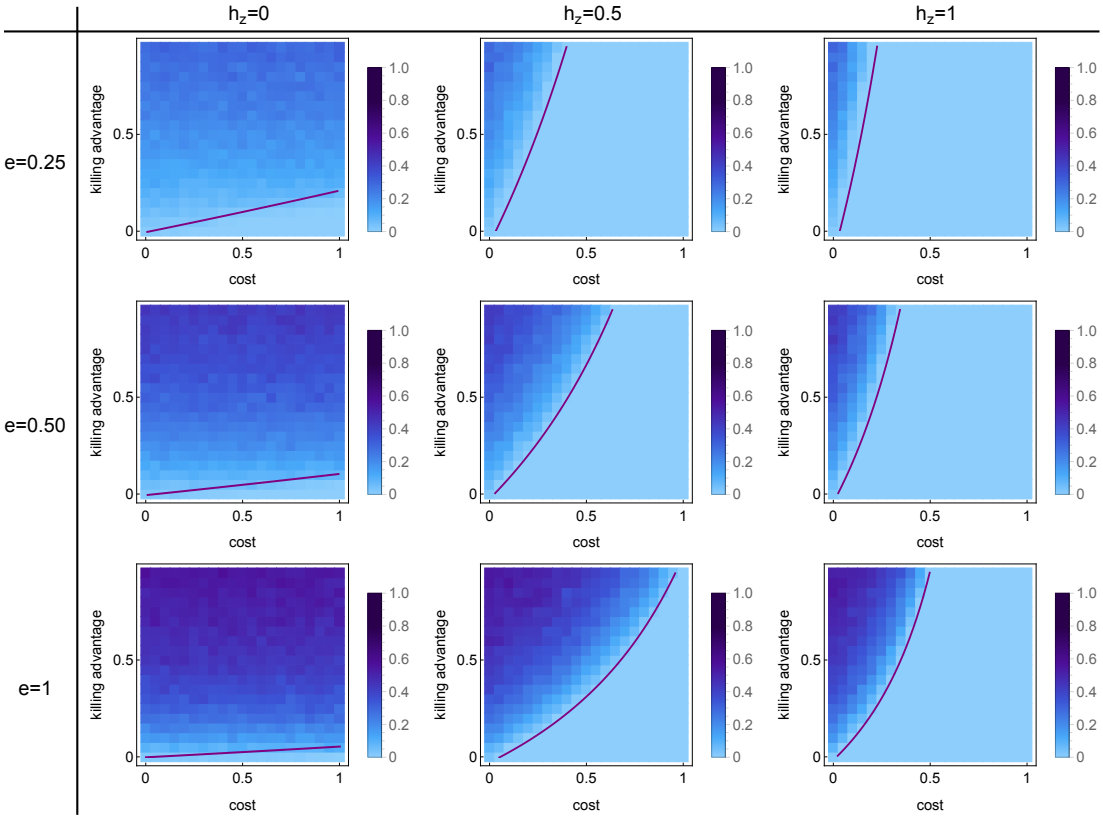

Figure 8: **Invasion probability of a spore killer with diploid fitness cost in *Neurospora* as a function of killing advantage.** Each heatmap presents invasion probability of a spore killer allele as a function of fitness cost of carrying the allele (x-axis) and killing advantage a (y-axis). For each pixel, invasion probability is estimated from 10^3 stochastic simulations. The population size is 1000. Heatmaps are given for three values of killing efficiency e and three values of the dominance parameter of the diploid cost h_z. The purple line delineates the region of the parameter space that allows for invasion of the spore killer according to the deterministic analysis of the model (purple line from Supplementary figure S1), with invasion possible on the left side of the line.

4 Discussion

In the present study, we explore several aspects of the complexity of fungal life cycles and show how they affect the conditions under which a spore killing allele can invade and coexist with a non-killing allele. Our models describe in detail ascus composition (see Figure 1), which is crucial to the process of spore killing. This mechanistic aspect of our study reveals a predominant role of killing advantage in spore killer dynamics. Another novel aspect of our study is the development of stochastic models investigating invasion probability, which to our knowledge is the first effort of this kind in the study of spore killers. We based our model on a single allele responsible for both the spore killing and the resistance to spore killing, without allowing recombination between the two functions. This structure is consistent with the picture that is emerging from recent empirical studies of spore killers in several species of ascomycete fungi (Nuckolls et al., 2017; Hu et al., 2017; Vogan et al., 2019; Svedberg et al., 2020). The only other theoretical study of spore killing known to us (Nauta and Hoekstra, 1993) focused on the role of recombination between the killing and resistance functions, which was appropriate given what was known about the genetic architecture of spore killers at that time in *Neurospora*, but appears now to be the exception rather than the rule.

In the following sections, we first discuss general insights from our model about the invasion of spore killers, before discussing our results in the light of data from natural systems with particular attention to the spore killer systems *Spk-1* in *Neurospora* and *Spok* in *Podopsora* that inspired our models. Throughout, we put our findings in perspective to theoretical and empirical results from male and female meiotic drivers in animals and plants.

4.1 Spore killers in theory

4.1.1 Selective advantage and invasion of a spore killer

It is interesting to start with a comparison of the dynamics of spore killers in our model with the very general model by Hartl (1972) on sperm and pollen killers. In Hartl's model, gamete killers kill in the homozygote form (this could be seen as "self-killing" or "suicide" as effectively the killer allele eliminates other copies of itself). As a consequence, the advantage they get from killing is exactly cancelled out by the cost suffered in the homozygote form regardless of their frequency in the population. Such gamete killers obtain no selective advantage from just killing and remain neutral (true only for case A, no compensation in Hartl's 1972 model). In contrast, we know that spore killers do not "self-kill" in the homozygote form, which allows them to obtain simply by killing a positively frequency dependent selective advantage. We find (in agreement

with Nauta and Hoekstra, 1993) that this frequency dependent selective advantage tends to zero when the frequency of the spore killer becomes close to zero (for example when invading a very large population). The selective advantage of a spore killer will thus be minimal at the onset of invasion, and smaller the larger the population being invaded. Spore killers may therefore not be able to invade if any non-recessive fitness costs are associated with them, or simply in very large populations because the chances of stochastic loss early in the invasion are too high (though see Box 2). This feature clearly distinguishes spore killers from female drive systems (e.g. Hall and Dawe, 2018), in which the selective advantage due to meiotic drive alone may be enough to compensate for substantial fitness costs from the onset of the invasion.

On the other hand, although the invasion probability of a spore killer is substantially lower that that of a female driver, it is not negligible (Box 2). Moreover, owing to the frequency dependent nature of the spore killer's selective advantage, small or fragmented populations may represent easier targets for invasion; thus, the study of spore killers in structured populations, which we have only briefly addressed in Box 2, could represent an interesting prospect for future theoretical studies. In addition, we suggest that the invasion rate of spore killers could in fact increase with population size, as the inflation of the mutational supply of spore killers more than compensates for the decrease in the invasion probability of each individual spore killer. This last point is of course dependent on the mechanism of origin of spore killers, which we discuss in the next section.

In addition to the killing itself, we propose that spore killers could obtain killing advantage, i.e. a net fitness benefit from killing, either in the form of compensation or reduced local competition for resources. In Hartl's model 1972, compensation plays a crucial role as it is necessary for gamete killers to obtain a selective advantage at all. In the case of spore killers, we find that killing advantage is also crucial: although the spore killer obtains a selective advantage by killing alone, as we have seen this advantage is weak when the spore killer is at low frequency. Killing advantage, on the other hand, is not frequency dependent, and will benefit the spore killer as it invades from low frequency. As we have shown, killing advantage may be able to compensate for fitness costs associated with the spore killer, reducing the chance of stochastic loss and speeding up invasion. This means that it could be important for future empirical explorations of spore killers to determine whether killing advantage is present and to what extent, in order to better understand spore killer dynamics.

4.1.2 Coexistence of a spore killing allele with a non-killing allele

We also investigate the conditions for coexistence of a killing and non-killing allele. Meiotic drivers (MDs) are expected often to spread rapidly to fixation (Lindholm et al., 2016) instead

of coexisting with their non-driver alleles in stable polymorphisms, but when a MD is fixed it becomes undetectable. The MDs that are observed in natural conditions therefore likely exhibit the properties that allow them to be maintained in stable coexistence—understanding these properties is thus an important part of theoretical studies on meiotic drive. Classically, in male and female drive, a recessive fitness cost associated with the driving allele is required for coexistence (e.g. Hartl, 1970; Fishman and Kelly, 2015; Lewontin and Dunn, 1960; Holman et al., 2015). Coexistence occurs as the cost is mostly expressed in the homozygote form, which prevents fixation, but not in the heterozygote form, which allows for invasion. We find this behavior in our models for both *Neurospora* and *Podospora*. A fitness cost is needed for coexistence to be possible and recessive costs allow a larger parameter space for coexistence as seen in Figure 2 (also affected by killing efficiency, rate of first-division segregation and selfing rate). For coexistence to be possible it is also necessary that the spore killer does not kill with full efficiency, so that the sensitive allele can have a positive fitness when in a diploid heterozygote. Incomplete killing can happen if killing efficiency is not 100%, or if second-division segregation occurs in the case of *Podospora*.

We also find that coexistence is possible even if the fitness cost to the spore killer is not recessive, which seems surprising at first. Such coexistence occurs because non-killer spores that survive killing also benefit from the killing advantage. We believe that this assumption is reasonable given the two possible scenarios that we envision for killing advantage to occur, compensation and reduction in local competition. With compensation due to additional spores produced by the parent both killer spores and sensitive spores are produced (of course the sensitive spores would then be killed again in proportion to killing efficiency). If a killing advantage occurs through the removing of local competition with siblings, then the same reasoning applies and both types of surviving spores obtain a fitness advantage. Coexistence can occur in that case because the benefit to the surviving sensitive spores prevents fixation of the spore killer by raising the fitness of the sensitive allele in the heterozygote form above the fitness of the homozygote spore killer. We can therefore see that fundamentally the mechanism of coexistence does not differ from the recessive cost mechanism (or overdominance, Hartl, 1970), but that the underlying biology is truly a specificity of spore killers.

4.1.3 Mating system and spore killer dynamics

We find that the rate of selfing of the host can have important effects on the dynamics of the spore killer. Selfing acts by slowing down the transmission of the spore killer, which occurs through heterozygote individuals produced by outcrossing. Of course, inbreeding could in theory have the same effect as selfing, and spore killer models where the assumption of random mating

is relaxed could be a interesting next step for theoretical exploration. This effect of selfing also suggests that mating behavior itself, either through selfing or inbreeding, could evolve as a defence mechanism against spore killers, as suggested by Lewontin and Dunn (1960). Bull (2017) and Bull et al. (2019) have built models showing that inbreeding could evolve as an efficient response to costly meiotic drivers. Their result can also be linked to the model of Burt and Trivers 1998, which suggests with supporting data that obligatory outcrossers in plants may carry higher numbers of costly genomic parasites. In addition, if an intrinsic fitness cost is associated with the spore killer, its effect will be magnified by selfing because selfing slows down the invasion of the killer while the fitness cost remains unchanged. Because of this effect, we predict that a spore killer would be able to invade only with a very minimal fitness cost in a population where selfing rate is high, and that coexistence would then be unlikely. This second effect of selfing also supports the idea that it may play a role as a defence mechanism from the host against spore killers.

4.2 Insights from natural systems

4.2.1 How much do we know about spore killers in nature?

In several model systems of male and female drive, the molecular mechanism of the meiotic driver (MD), its fitness effects and the biology of the host are known to the extent that population genetics models can predict the frequency of the MD in natural or laboratory populations with impressive accuracy. For example, Fishman and Kelly (2015) could predict the equilibrium value of a female drive in populations of the monkeyflower *Mimulus guttatus*, knowing the transmission advantage of the MD and its associated costs to male fertility and to female fitness. Similarly, working on the *t-haplotype* in the mouse *Mus musculus*, Lewontin and Dunn (1960) were able to integrate accurate transmission rate measured from the biological model, viability effects of the MD, as well as realistic population structure and mating behavior and were successful at predicting observed frequencies of the MD. In the case of spore killers, however, although several recent papers shed light on the genetic and molecular basis of their driving action (Vogan et al., 2019; Svedberg et al., 2020; Nuckolls et al., 2017; Hu et al., 2017), many unknowns remain, particularly regarding the ecology of the hosts, making accurate predictions difficult. In this section, we summarize the available knowledge and use it to put results from our models in perspective and to suggest future directions for empirical research.

We focus on the three spore killers in fungal hosts that are best understood: the *Spok* gene family in *Podospora anserina* (Vogan et al., 2019) and *Spk-1* in *Neurospora sitophila* (Svedberg et al., 2020), both of which directly inspired our models, and the *wtf* gene family in *Schizosaccha-*

romyces pombe (Hu et al., 2017; Nuckolls et al., 2017), which is also well studied and has many similarities with the two first ones. In all three examples, resistance and spore killing are due to a single allele and thus match our model assumption on the genetic architecture.

Little is known about the origin of spore killers. It has been proposed that spore killing systems may arise neutrally in populations in which resistance to killing has been fixed first, just like any other incompatibility system between diverging populations (Sweigart et al., 2019). However, our work shows that an active spore killer has greater a chance of invading than a neutral allele, which supports the view of selfish evolution of spore killers. *Spoks*, *Spk-1* and *wtf* all belong to large families of genes that occur across complexes of closely related fungal species or clades (genetically diverged groups). In each of the above gene families some members are active killers while others seem to only confer resistance to killing or else are completely inactive. This suggests a history of coevolution with the host or an ability to transfer horizontally across populations. For example, there is evidence that *Spk-1* in *N. sitophila* may have introgressed from the closely related *N. hispaniola* (Svedberg et al., 2020). The landscape of spore killer gene families across fungal species also points to the possibility that spore killers are derived from genes with an adaptive function in their host. Another possibility would be that these originally selfish genetic elements become domesticated over time by their host, as suggested by Werren (2011). *Spok* and *wtf* genes move and mutate rapidly (Vogan et al., 2019; Nuckolls et al., 2017; Hu et al., 2017). In *Podospora* in particular, the action of RIP, a cellular mechanism that targets duplicated genes with *de novo* mutations (Arnaise et al., 2008), could increase the mutation rate and accelerate the creation of new spore killers.

4.2.2 Insights from our models on spore killer dynamics in natural populations

The *Spok* genes in *Podospora anserina*, *Spok2*, *Spok3* and *Spok4*, do not all behave the same. Supplementary figure S16 shows the frequency of these *Spok* genes in samples of *P. anserina* over a 17 years period. None of the spore killers reached complte fixation or went extinct during that period. However we can see that *Spok2* appears close to fixation while *Spok3* and *Spok4* are at lower frequency. *Spok2* occurs at higher frequency regardless of the fact that at least *Spok4* kills with 100% efficiency while *Spok2* does not (Vogan et al., 2019). On the other hand, *Spok3* and *Spok4* are integrated within a larger genomic element known as the "*Spok* block" (Vogan et al., 2019), which could associate a fitness cost to these alleles explaining their lower frequency relative to *Spok2*. *P. anserina* is expected to engage in selfing frequently, although there is clear evidence for outcrossing as well (van der Gaag, 2005; Vogan et al., 2019). Because of the high selfing rate, fitness costs may better explain the behavior of the different *Spok* genes than their killing

efficiency, in agreement with our model's results.

The *Spk-1* killer of *N. sitophila* shows population structure, being respectively fixed and absent in two clades that coexist in sympatry and polymorphic in a third clade, where a form of resistance to the killer has evolved (Svedberg et al., 2020). This suggests that the dynamics of a same spore killer may follow very different routes in different populations, and investigating further why this occurred should bring insights on spore killer dynamics.

Unfortunately, very little is known about the frequency of *wtf* alleles in natural populations of *S. pombe* and we can only speculate from the little information that we have. We know that killing efficiency is lower than 100% (Nuckolls et al., 2017; Núñez et al., 2020), that *S. pombe* is likely selfing at high rates (Tusso et al., 2019; Nieuwenhuis and James, 2016), and able to perform haploid selfing, something not possible in our *Podospora* model. Based on this information, we predict that the fitness costs of *wtf* must be low to allow for invasion, that invading spore killers progress slowly and are sensitive to stochastic loss or the evolution of suppressors (alleles counteracting the action of the spore killer).

At least one supressor counteracting the action of the spore killer has evolved in *S. pombe* (Nuckolls et al., 2017; Núñez et al., 2020), and there is also evidence for suppression in the clade of *N. sitophila* in which polymorphism is observed. Suppressor genes are likely to evolve if given enough time (slow invasion or stable coexistence) and are found in many other drive systems, but in *P. anserina* so far (Vogan et al., 2019).

The spore killers that we discuss here, *Spk-1*, *Spok* and *wtf* are all small genomic regions without inversions, suggesting that they may not be associated with hitchhiking deleterious mutations. At the same time, they all function with a poison-antidote mechanism, that could easily be associated with a cost, potentially recessive if subject to a dosage effect. As to date, there is no definitive evidence for or against a fitness cost of carrying these spore killers. Similarly, although we have proposed what we think are reasonable scenarios for killing advantage, there is no empirical evidence yet to argue for its presence or absence.

4.2.3 Spore killers and diversification of their hosts

The two coexisting clades in which *Spk-1* is either fixed or absent are apparently reproductively isolated in the wild, and this raises the question of whether the spore killer itself could have played a role in this isolation. This idea can be paralleled to the case of *wtf*, which is suggested to have contributed to the rapid diversification of the *S. pombe* family (Hu et al., 2017). An effect of spore killers on diversification of their hosts would not be surprising as in general meiotic drivers are thought to play a role in speciation by creating incompatibilities between recently diverged

populations (Lindholm et al., 2016) as is the case for example in *Drosophila* (Phadnis and Orr, 2009; Zhang et al., 2015).

4.3 Conclusion

In conclusion, compared to other meiotic drive systems there remains many unknowns with spore killers. Fitness costs, killing advantage, host population size and mating system are parameters that are, according to our model, important for the dynamics of spore killers. Yet, these parameters are not well understood in the three species that we discussed. In recent years, empirical efforts have unveiled a wealth of new knowledge about these spore killers, and we hope that this trend will continue. An important task will be to better characterize the mating systems of fungal hosts (Nieuwenhuis and James, 2016), as we have seen its importance for spore killer dynamics. According to our models, we predict that there should be similarities between spore killers well-studied systems of meiotic drive. We expect for example fitness costs (likely but not necessarily recessive) to explain coexistence. Moreover, spore killers may play a role in population divergence, maybe speciation, as evidence suggests for both *wtf* and *Spk-1*. In any case, a better knowledge of spore killers is needed as the advent of artificial meiotic drive opens up a world of possibilities for biological control of fungal species Lindholm et al. (2016); Esvelt et al. (2014), which could also become a Pandora box if not well understood.

References

Akbari, O. S., K. D. Matzen, J. M. Marshall, H. Huang, C. M. Ward, and B. A. Hay. 2013. A synthetic gene drive system for local, reversible modification and suppression of insect populations. Current Biology 23:671–677.

Arnaise, S., D. Zickler, A. Bourdais, M. Dequard-Chablat, and R. Debuchy. 2008. Mutations in mating-type genes greatly decrease repeat-induced point mutation process in the fungus podospora anserina. Fungal genetics and biology 45:207–220.

Brand, C. L., A. M. Larracuente, and D. C. Presgraves. 2015. Origin, evolution, and population genetics of the selfish segregation distorter gene duplication in european and african populations of drosophila melanogaster. Evolution 69:1271–1283.

Buckler, E. S., T. L. Phelps-Durr, C. S. K. Buckler, R. K. Dawe, J. F. Doebley, and T. P. Holtsford. 1999. Meiotic drive of chromosomal knobs reshaped the maize genome. Genetics 153:415–426.

Bull, J. J. 2017. Lethal gene drive selects inbreeding. Evolution, medicine, and public health 2017:1–16.

Bull, J. J., C. H. Remien, and S. M. Krone. 2019. Gene-drive-mediated extinction is thwarted by evolution of sib mating. bioRxiv page 558924.

Burt, A., and R. Trivers. 1998. Selfish dna and breeding system in flowering plants. Proceedings of the Royal Society of London. Series B: Biological Sciences 265:141–146.

———. 2006. Genes in conflict: the biology of selfish genetic elements. Harvard University Press, Cambridge.

Charlesworth, B., and D. L. Hartl. 1978. Population dynamics of the segregation distorter polymorphism of drosophila melanogaster. Genetics 89:171–192.

Crow, J. F. 1991. Why is mendelian segregation so exact? BioEssays 13:305–312.

Desai, M. M., and D. S. Fisher. 2007. Beneficial mutation–selection balance and the effect of linkage on positive selection. Genetics 176:1759–1798.

Didion, J. P., A. P. Morgan, A. M.-F. Clayshulte, R. C. Mcmullan, L. Yadgary, P. M. Petkov, T. A. Bell, D. M. Gatti, J. J. Crowley, K. Hua, et al. 2015. A multi-megabase copy number gain causes maternal transmission ratio distortion on mouse chromosome 2. PLoS genetics 11:e1004850.

Esser, K. 1974. Podospora anserina. Pages 531–551 *in* Bacteria, Bacteriophages, and Fungi. Springer.

Esvelt, K. M., A. L. Smidler, F. Catteruccia, and G. M. Church. 2014. Emerging technology: concerning rna-guided gene drives for the alteration of wild populations. Elife 3:e03401.

Fishman, L., and J. K. Kelly. 2015. Centromere-associated meiotic drive and female fitness variation in mimulus. Evolution 69:1208–1218.

Fishman, L., and A. Saunders. 2008. Centromere-associated female meiotic drive entails male fitness costs in monkeyflowers. Science 322:1559–1562.

Frank, S. A. 1991. Divergence of meiotic drive-suppression systems as an explanation for sex-biased hybrid sterility and inviability. Evolution 45:262–267.

Gale, J. S. 1990. Theoretical Population Genetics. Unwin Hyman, London.

Haig, D., and C. T. Bergstrom. 1995. Multiple mating, sperm competition and meiotic drive. Journal of Evolutionary Biology 8:265–282.

Hall, D. W., and R. K. Dawe. 2018. Modeling the evolution of female meiotic drive in maize. G3: Genes, Genomes, Genetics 8:123–130.

Hamilton, W. D. 1967. Extraordinary sex ratios. Science 156:477–488.

Hartl, D. 1970. Analysis of a general population genetic model of meiotic drive. Evolution pages 538–545.

Hartl, D. L. 1972. Population dynamics of sperm and pollen killers. Theoretical and Applied Genetics 42:81–88.

Henikoff, S., K. Ahmad, and H. S. Malik. 2001. The centromere paradox: stable inheritance with rapidly evolving dna. Science 293:1098–1102.

Hiraizumi, Y. 1962. Distorted segregation and genetic load. The Japanese Journal of Genetics 37:147–154.

Holman, L., T. A. Price, N. Wedell, and H. Kokko. 2015. Coevolutionary dynamics of polyandry and sex-linked meiotic drive. Evolution 69:709–720.

Holsinger, K. E., M. W. Feldman, and F. B. Christiansen. 1984. The evolution of self-fertilization in plants: a population genetic model. The American Naturalist 124:446–453.

Hu, W., Z.-D. Jiang, F. Suo, J.-X. Zheng, W.-Z. He, and L.-L. Du. 2017. A large gene family in fission yeast encodes spore killers that subvert mendel's law. Elife 6:e26057.

Hurst, G. D., and J. H. Werren. 2001. The role of selfish genetic elements in eukaryotic evolution. Nature Reviews Genetics 2:597.

Kimura, M. 1962. On the probability of fixation of mutant genes in a population. Genetics 47:713–719.

Kyrou, K., A. M. Hammond, R. Galizi, N. Kranjc, A. Burt, A. K. Beaghton, T. Nolan, and A. Crisanti. 2018. A crispr–cas9 gene drive targeting doublesex causes complete population suppression in caged anopheles gambiae mosquitoes. Nature biotechnology 36:1062.

Larracuente, A. M., and D. C. Presgraves. 2012. The selfish segregation distorter gene complex of drosophila melanogaster. Genetics 192:33–53.

Lewontin, R. C. 1968. The effect of differential viability on the population dynamics of t alleles in the house mouse. Evolution pages 262–273.

Lewontin, R. C., and L. C. Dunn. 1960. The evolutionary dynamics of a polymorphism in the house mouse. Genetics 45:705–722. Cited By :110.

Lindholm, A. K., K. A. Dyer, R. C. Firman, L. Fishman, W. Forstmeier, L. Holman, H. Johannesson, U. Knief, H. Kokko, A. M. Larracuente, et al. 2016. The ecology and evolutionary dynamics of meiotic drive. Trends in ecology & evolution 31:315–326.

Lyttle, T. W. 1991. Segregation distorters. Annual review of genetics 25:511–581.

———. 1993. Cheaters sometimes prosper: distortion of mendelian segregation by meiotic drive. Trends in Genetics 9:205–210.

Meade, L. C., D. Dinneen, R. Kad, D. M. Lynch, K. Fowler, and A. Pomiankowski. 2019. Ejaculate sperm number compensation in stalk-eyed flies carrying a selfish meiotic drive element. Heredity 122:916.

Nauta, M. J., and R. F. Hoekstra. 1993. Evolutionary dynamics of spore killers. Genetics 135:923–930.

Nieuwenhuis, B. P., and T. Y. James. 2016. The frequency of sex in fungi. Philosophical Transactions of the Royal Society B: Biological Sciences 371:20150540.

Nuckolls, N. L., M. A. B. Núñez, M. T. Eickbush, J. M. Young, J. J. Lange, S. Y. Jonathan, G. R. Smith, S. L. Jaspersen, H. S. Malik, and S. E. Zanders. 2017. wtf genes are prolific dual poison-antidote meiotic drivers. Elife 6:e26033.

Núñez, M. A. B., I. M. Sabbarini, M. T. Eickbush, Y. Liang, J. J. Lange, A. M. Kent, and S. E. Zanders. 2020. Dramatically diverse schizosaccharomyces pombe wtf meiotic drivers all display high gamete-killing efficiency. PLoS Genetics 16:e1008350.

Otto, S. P., and T. Day. 2011. A biologist's guide to mathematical modeling in ecology and evolution. Princeton University Press, Princeton.

Padieu, E., and J. Bernet. 1967. Mode d'action des gènes responsables de l'avortement de certains produits de la méiose chez l'ascomycète *Podospora anserina*. Compte Rendu Hebdomadaire des Séances de l'Académie des Sciences Série D:2300–2303.

Phadnis, N., and H. A. Orr. 2009. A single gene causes both male sterility and segregation distortion in drosophila hybrids. science 323:376–379.

Pinzone, C. A., and K. A. Dyer. 2013. Association of polyandry and sex-ratio drive prevalence in natural populations of drosophila neotestacea. Proceedings of the Royal Society B: Biological Sciences 280:20131397.

Raju, N. B. 1994. Ascomycete spore killers: chromosomal elements that distort genetic ratios among the products of meiosis. Mycologia 86:461–473.

Rhoades, M. 1942. Preferential segregation in maize. Genetics 27:395.

Rice, W. R. 2013. Nothing in genetics makes sense except in light of genomic conflict. Annual Review of Ecology, Evolution, and Systematics 44:217–237.

Sandler, L., and E. Novitski. 1957. Meiotic drive as an evolutionary force. The American Naturalist 91:105–110.

Silar, P. 2013. Podospora anserina: from laboratory to biotechnology. Pages 283–309 *in* Genomics of Soil-and Plant-Associated Fungi. Springer.

Silver, L. M. 1985. Mouse tau haplotypes. Annual review of genetics 19:179–208.

Svedberg, J., A. A. Vogan, N. A. Rhoades, D. Sarmarajeewa, D. J. Jacobson, M. Lascoux, T. M. Hammond, and H. Johannesson. 2020. An introgressed gene causes meiotic drive in neurospora sitophila. bioRxiv .

Sweigart, A. L., Y. Brandvain, and L. Fishman. 2019. Making a murderer: the evolutionary framing of hybrid gamete-killers. Trends in Genetics .

Turner, B. C., and D. D. Perkins. 1979. Spore killer, a chromosomal factor in neurospora that kills meiotic products not containing it. Genetics 93:587–606.

Tusso, S., B. P. Nieuwenhuis, F. J. Sedlazeck, J. W. Davey, D. C. Jeffares, and J. B. Wolf. 2019. Ancestral admixture is the main determinant of global biodiversity in fission yeast. Molecular biology and evolution 36:1975–1989.

van der Gaag, M. 2005. Genomic conflicts in Podospora anserina= Genomische conflicten in Podospora anserina. Thesis Wageningen University.

van der Gaag, M., A. J. Debets, J. Oosterhof, M. Slakhorst, J. A. Thijssen, and R. F. Hoekstra. 2000. Spore-killing meiotic drive factors in a natural population of the fungus podospora anserina. Genetics 156:593–605.

Vogan, A. A., S. L. Ament-Velásquez, A. Granger-Farbos, J. Svedberg, E. Bastiaans, A. J. Debets, V. Coustou, H. Yvanne, C. Clavé, S. J. Saupe, et al. 2019. Combinations of spok genes create multiple meiotic drivers in podospora. Elife 8.

Werren, J. H. 2011. Selfish genetic elements, genetic conflict, and evolutionary innovation. Proceedings of the National Academy of Sciences 108:10863–10870.

Zanders, S. E., M. T. Eickbush, S. Y. Jonathan, J.-W. Kang, K. R. Fowler, G. R. Smith, and H. S. Malik. 2014. Genome rearrangements and pervasive meiotic drive cause hybrid infertility in fission yeast. Elife 3:e02630.

Zhang, L., T. Sun, F. Woldesellassie, H. Xiao, and Y. Tao. 2015. Sex ratio meiotic drive as a plausible evolutionary mechanism for hybrid male sterility. PLoS genetics 11.

Supplementary Material

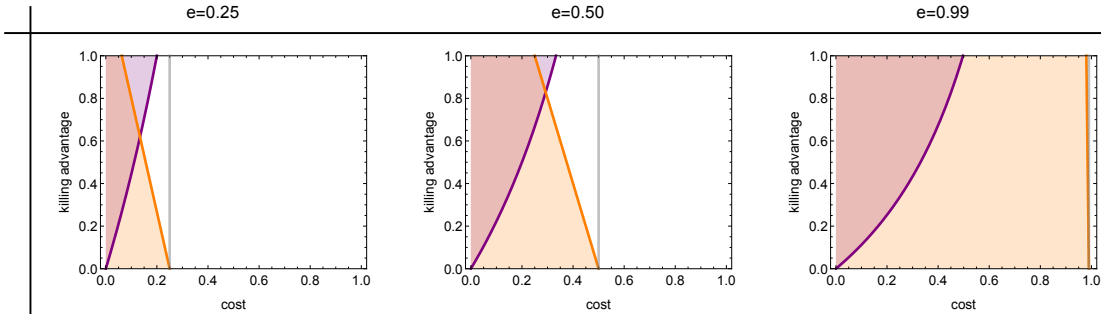

Figure S1: **Haploid cost: parameter space allowing stable polymorphism of the spore killer in *Neurospora*.** Each graph is given for a different value of killing efficiency of the spore killer (e). The intensity of the haploid cost is represented on the x-axis of each graph and the degree of killing advantage during spore killing (a) on the y-axis. The area above the purple line represents the parameter space where the spore killer can invade a population, starting from a frequency close to zero (corresponding to condition $L_D > 1$). To the left of the orange line is the parameter space where the spore killer can go to fixation when close to a frequency of one (corresponding to condition $L_d > L_{DD}$). A stable polymorphism is possible when the spore killer can invade (above the purple line) but not go to fixation (on the right of the orange line). This space is larger when killing efficiency is low. The white area represents the parameter space where the spore killer is simply unable to invade or fix. The red-shaded area represents the parameter space where the spore killer can invade and goes to fixation. Finally, the yellow-shaded space represents the parameter space where the spore killer could eventually reach fixation from intermediate frequencies but is not allowed to invade. The grey line represents the position the orange line would occupy if sensitive spores surviving killing would not benefit from killing advantage. We can see that in that last case, no stable polymorphism is possible with a haploid cost.

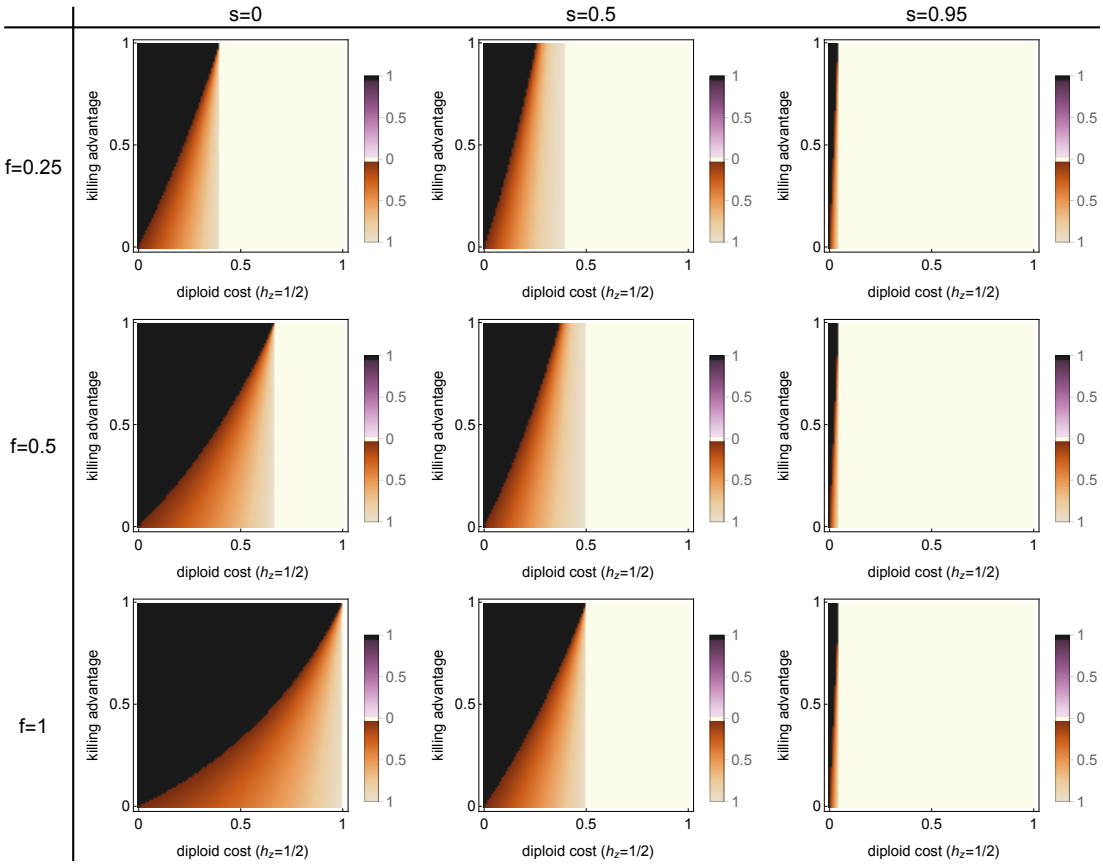

Figure S2: **Additive diploid fitness cost ($h_k = 1/2$). Equilibrium values and stability of the spore killer in *Podospora*, as a function of fitness cost, selfing rate (s), rate of first-division segregation (f) and killing advantage.** Equilibrium value and stability were determined by solving the equation system that defines the model for Podospora. Each graph gives equilibrium values for 100 values of fitness cost and 100 values of compensation. White cells correspond to $p_D = 0$ being a stable equilibrium and $p_D = 1$ being the only other (unstable) equilibrium. In these cases the spore killer cannot invade. Black cells correspond to $p_D = 1$ being a stable equilibrium with $p_D = 0$ being the only other (unstable) equilibrium, which means that the spore killer can invade and goes to fixation. Shades of purple indicate a stable internal equilibrium, which value is indicated by the scale next to each plot, with both $p_D = 0$ and $p_D = 1$ unstable. In that case, the spore killer can invade but will not reach fixation, a stable polymorphism can exist. Finally, shades of brown represent an unstable internal equilibrium, with the value of the equilibrium frequency indicated by the shade of brown on the scale besides each plot. In that case, both $p_D = 0$ and $p_D = 1$ are stable, meaning that the spore killer shouldn't be able to invade, but if present in the population at a frequency higher than the unstable equilibrium, it can then reach fixation.

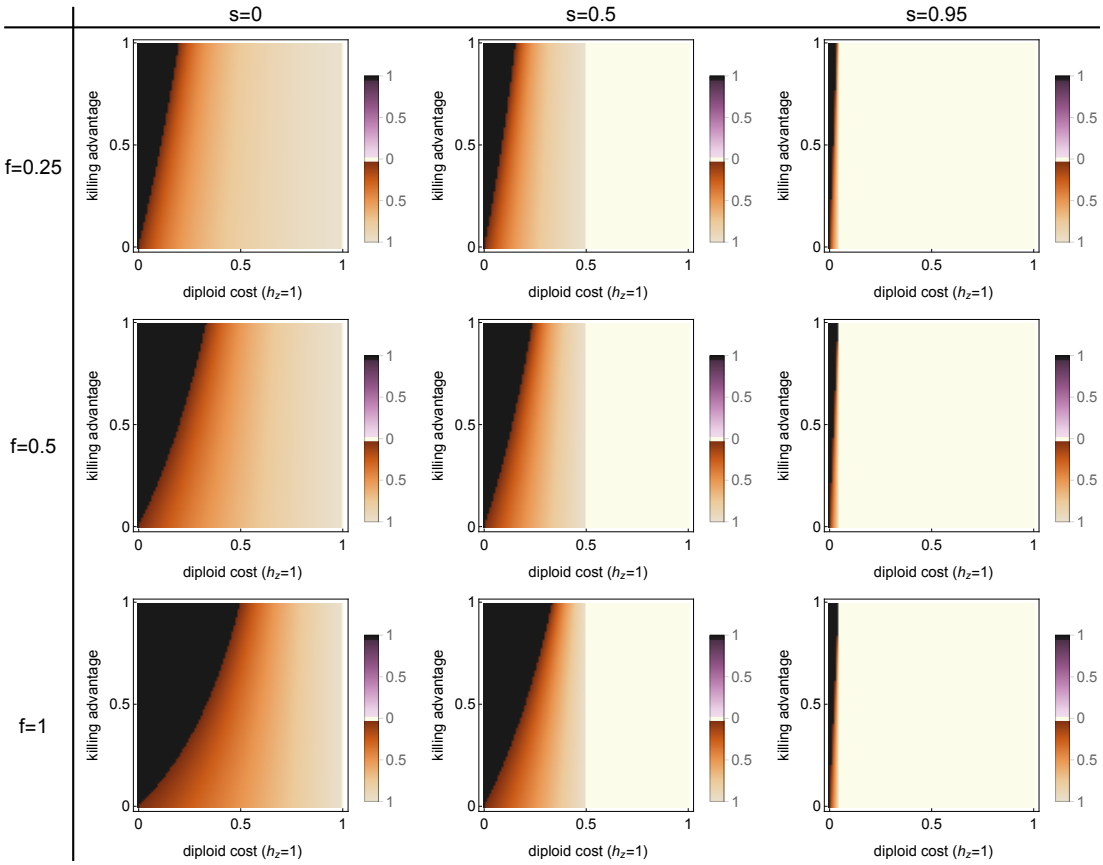

Figure S3: **Dominant diploid fitness cost ($hz = 1$).Equilibrium values and stability of the spore killer in *Podospora*, as a function of fitness cost, selfing rate (s), rate of first-division segregation (f) and killing advantage.** Equilibrium value and stability were determined by solving the equation system that defines the model for Podospora. Each graph gives equilibrium values for 100 values of fitness cost and 100 values of compensation. White cells correspond to $p_D = 0$ being a stable equilibrium and $p_D = 1$ being the only other (unstable) equilibrium. In these cases the spore killer cannot invade. Black cells correspond to $p_D = 1$ being a stable equilibrium with $p_D = 0$ being the only other (unstable) equilibrium, which means that the spore killer can invade and goes to fixation. Shades of purple indicate a stable internal equilibrium, which value is indicated by the scale next to each plot, with both $p_D = 0$ and $p_D = 1$ unstable. In that case, the spore killer can invade but will not reach fixation, a stable polymorphism can exist. Finally, shades of brown represent an unstable internal equilibrium, with the value of the equilibrium frequency indicated by the shade of brown on the scale besides each plot. In that case, both $p_D = 0$ and $p_D = 1$ are stable, meaning that the spore killer shouldn't be able to invade, but if present in the population at a frequency higher than the unstable equilibrium, it can then reach fixation.

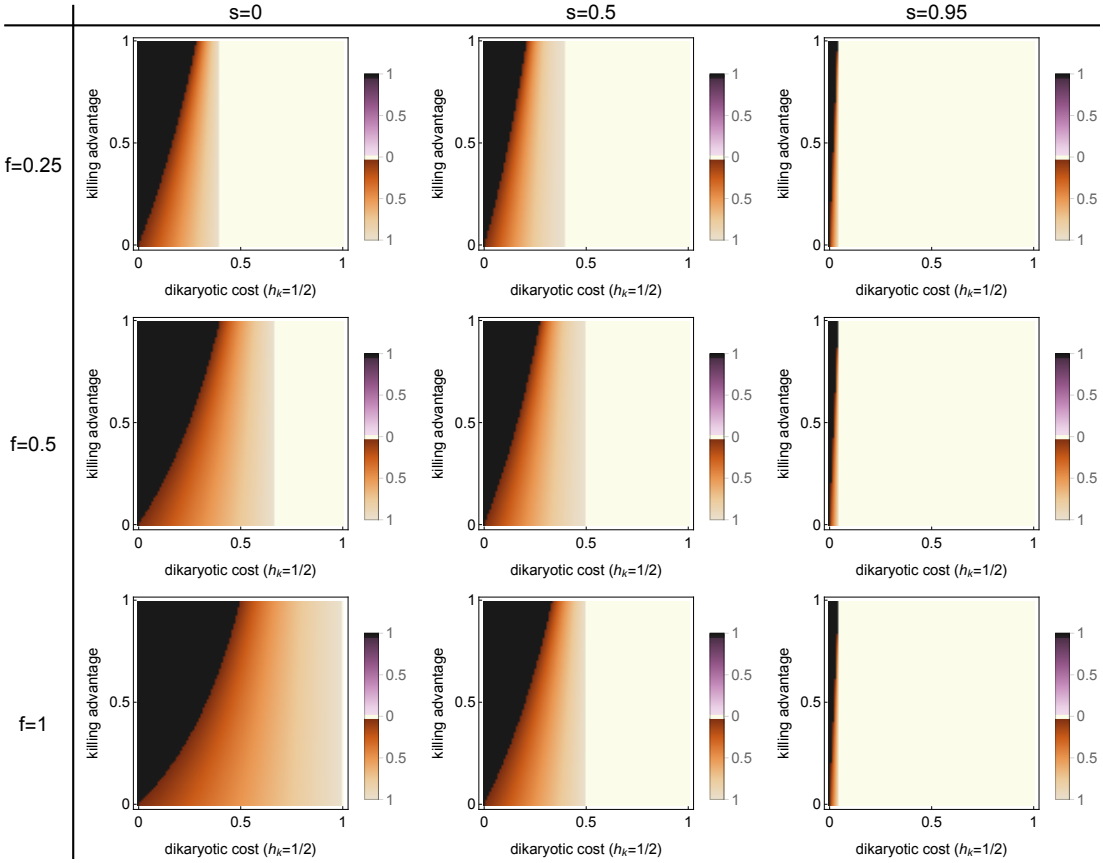

Figure S4: **Additive dikaryotic fitness cost (h_k=1/2). Equilibrium values and stability of the spore killer in *Podospora*, as a function of fitness cost, selfing rate (s), rate of first-division segregation (f) and killing advantage.** Equilibrium value and stability were determined by solving the equation system that defines the model for Podospora. Each graph gives equilibrium values for 100 values of fitness cost and 100 values of compensation. White cells correspond to $p_D = 0$ being a stable equilibrium and $p_D = 1$ being the only other (unstable) equilibrium. In these cases the spore killer cannot invade. Black cells correspond to $p_D = 1$ being a stable equilibrium with $p_D = 0$ being the only other (unstable) equilibrium, which means that the spore killer can invade and goes to fixation. Shades of purple indicate a stable internal equilibrium, which value is indicated by the scale next to each plot, with both $p_D = 0$ and $p_D = 1$ unstable. In that case, the spore killer can invade but will not reach fixation, a stable polymorphism can exist. Finally, shades of brown represent an unstable internal equilibrium, with the value of the equilibrium frequency indicated by the shade of brown on the scale besides each plot. In that case, both $p_D = 0$ and $p_D = 1$ are stable, meaning that the spore killer shouldn't be able to invade, but if present in the population at a frequency higher than the unstable equilibrium, it can then reach fixation.

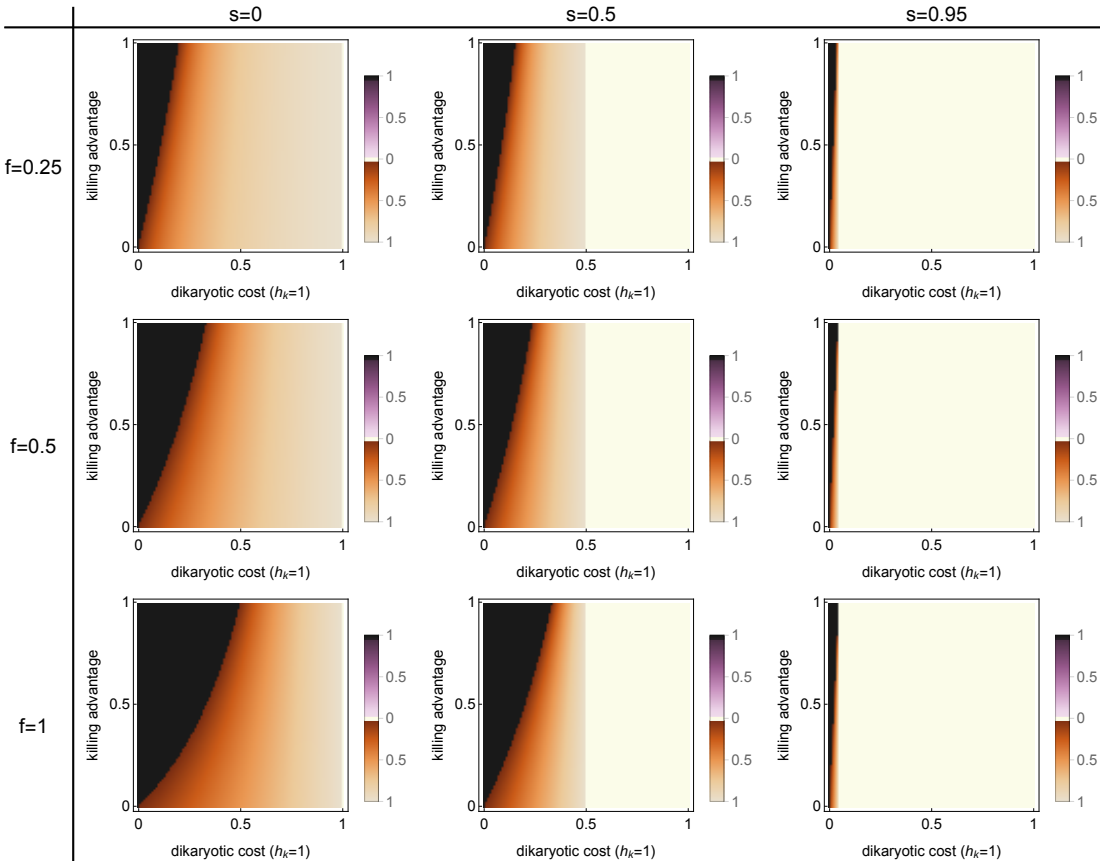

Figure S5: **Dominant dikaryotic fitness cost ($h_k = 1$). Equilibrium values and stability of the spore killer in *Podospora*, as a function of fitness cost, selfing rate (s), rate of first-division segregation (f) and killing advantage.** Equilibrium value and stability were determined by solving the equation system that defines the model for Podospora. Each graph gives equilibrium values for 100 values of fitness cost and 100 values of compensation.White cells correspond to $p_D = 0$ being a stable equilibrium and $p_D = 1$ being the only other (unstable) equilibrium. In these cases the spore killer cannot invade. Black cells correspond to $p_D = 1$ being a stable equilibrium with $p_D = 0$ being the only other (unstable) equilibrium, which means that the spore killer can invade and goes to fixation. Shades of purple indicate a stable internal equilibrium, which value is indicated by the scale next to each plot, with both $p_D = 0$ and $p_D = 1$ unstable. In that case, the spore killer can invade but will not reach fixation, a stable polymorphism can exist. Finally, shades of brown represent an unstable internal equilibrium, with the value of the equilibrium frequency indicated by the shade of brown on the scale besides each plot. In that case, both $p_D = 0$ and $p_D = 1$ are stable, meaning that the spore killer shouldn't be able to invade, but if present in the population at a frequency higher than the unstable equilibrium, it can then reach fixation.

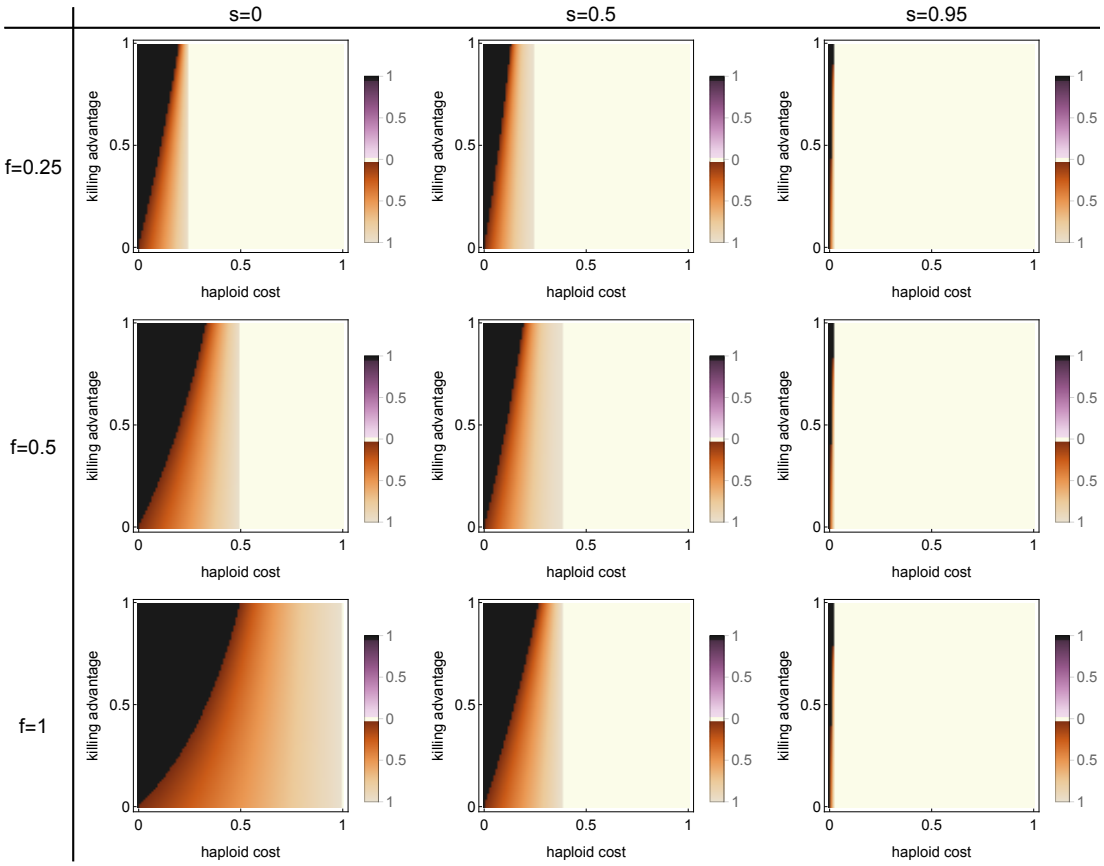

Figure S6: **Haploid fitness cost. Equilibrium values and stability of the spore killer in *Podospora*, as a function of fitness cost, selfing rate (s), rate of first-division segregation (f) and killing advantage.** Equilibrium value and stability were determined by solving the equation system that defines the model for Podospora. Each graph gives equilibrium values for 100 values of fitness cost and 100 values of killing advantage. White cells correspond to $p_D = 0$ being a stable equilibrium and $p_D = 1$ being the only other (unstable) equilibrium. In these cases the spore killer cannot invade. Black cells correspond to $p_D = 1$ being a stable equilibrium with $p_D = 0$ being the only other (unstable) equilibrium, which means that the spore killer can invade and goes to fixation. Shades of purple indicate a stable internal equilibrium, which value is indicated by the scale next to each plot, with both $p_D = 0$ and $p_D = 1$ unstable. In that case, the spore killer can invade but will not reach fixation, a stable polymorphism can exist. Finally, shades of brown represent an unstable internal equilibrium, with the value of the equilibrium frequency indicated by the shade of brown on the scale besides each plot. In that case, both $p_D = 0$ and $p_D = 1$ are stable, meaning that the spore killer shouldn't be able to invade, but if present in the population at a frequency higher than the unstable equilibrium, it can then reach fixation.

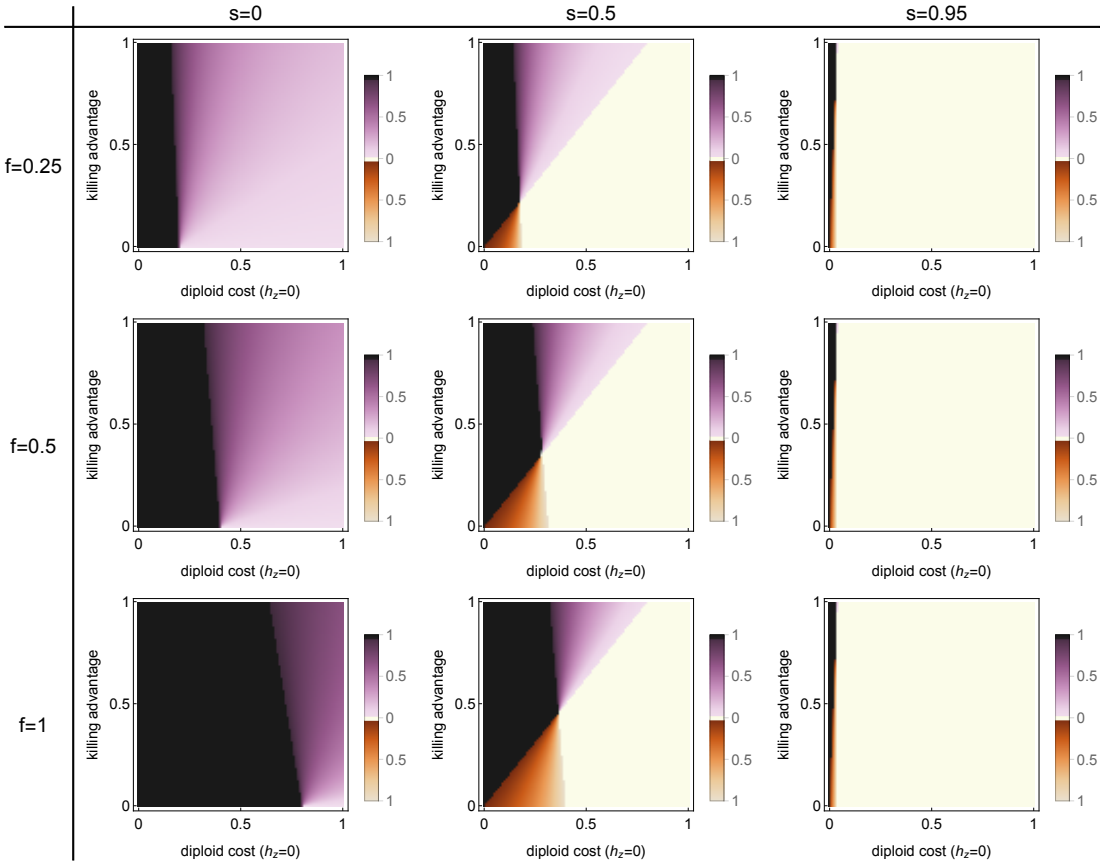

Figure S7: **Incomplete killing ($e = 0.8$) and recessive diploid fitness cost ($h_z = 0$). Equilibrium values and stability of the spore killer in *Podospora*, as a function of fitness cost, selfing rate (s), rate of first-division segregation (f) and killing advantage.** This figure can be compared to Figure 2 to see the effect of incomplete killing ($e = 0.8$ here) in *Podospora*. Equilibrium value and stability were determined by solving the equation system that defines the model for Podospora. Each graph gives equilibrium values for 100 values of fitness cost and 100 values of killing advantage. White cells correspond to $p_D = 0$ being a stable equilibrium and $p_D = 1$ being the only other (unstable) equilibrium. In these cases the spore killer cannot invade. Black cells correspond to $p_D = 1$ being a stable equilibrium with $p_D = 0$ being the only other (unstable) equilibrium, which means that the spore killer can invade and goes to fixation. Shades of purple indicate a stable internal equilibrium, which value is indicated by the scale next to each plot, with both $p_D = 0$ and $p_D = 1$ unstable. In that case, the spore killer can invade but will not reach fixation, a stable polymorphism can exist. Finally, shades of brown represent an unstable internal equilibrium, with the value of the equilibrium frequency indicated by the shade of brown on the scale besides each plot. In that case, both $p_D = 0$ and $p_D = 1$ are stable, meaning that the spore killer shouldn't be able to invade, but if present in the population at a frequency higher than the unstable equilibrium, it can then reach fixation.

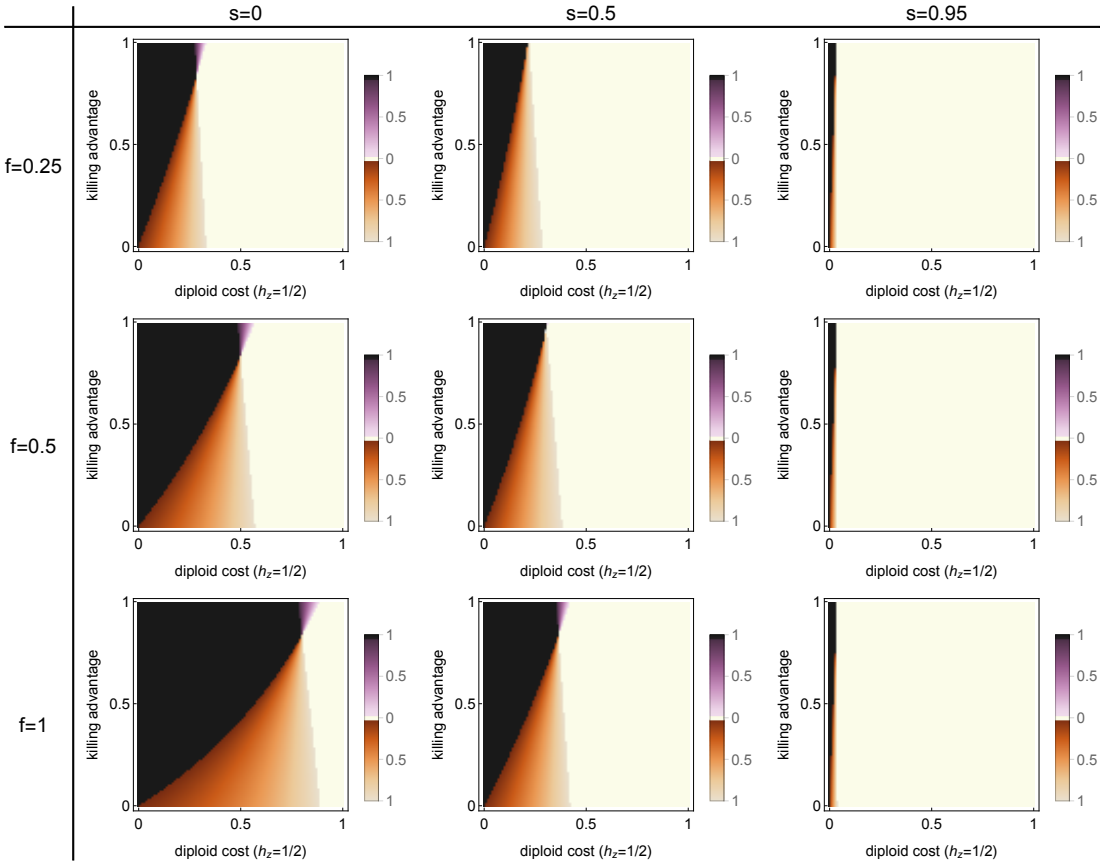

Figure S8: **Incomplete killing ($e = 0.8$) and additive diploid fitness cost ($h_z = 1/2$). Equilibrium values and stability of the spore killer in *Podospora*, as a function of fitness cost, selfing rate (s), rate of first-division segregation (f) and killing advantage.** This figure can be compared to Figure S2 to see the effect of incomplete killing ($e = 0.8$ here) in *Podospora*. Equilibrium value and stability were determined by solving the equation system that defines the model for Podospora. Each graph gives equilibrium values for 100 values of fitness cost and 100 values of killing advantage. White cells correspond to $p_D = 0$ being a stable equilibrium and $p_D = 1$ being the only other (unstable) equilibrium. In these cases the spore killer cannot invade. Black cells correspond to $p_D = 1$ being a stable equilibrium with $p_D = 0$ being the only other (unstable) equilibrium, which means that the spore killer can invade and goes to fixation. Shades of purple indicate a stable internal equilibrium, which value is indicated by the scale next to each plot, with both $p_D = 0$ and $p_D = 1$ unstable. In that case, the spore killer can invade but will not reach fixation, a stable polymorphism can exist. Finally, shades of brown represent an unstable internal equilibrium, with the value of the equilibrium frequency indicated by the shade of brown on the scale besides each plot. In that case, both $p_D = 0$ and $p_D = 1$ are stable, meaning that the spore killer shouldn't be able to invade, but if present in the population at a frequency higher than the unstable equilibrium, it can then reach fixation.

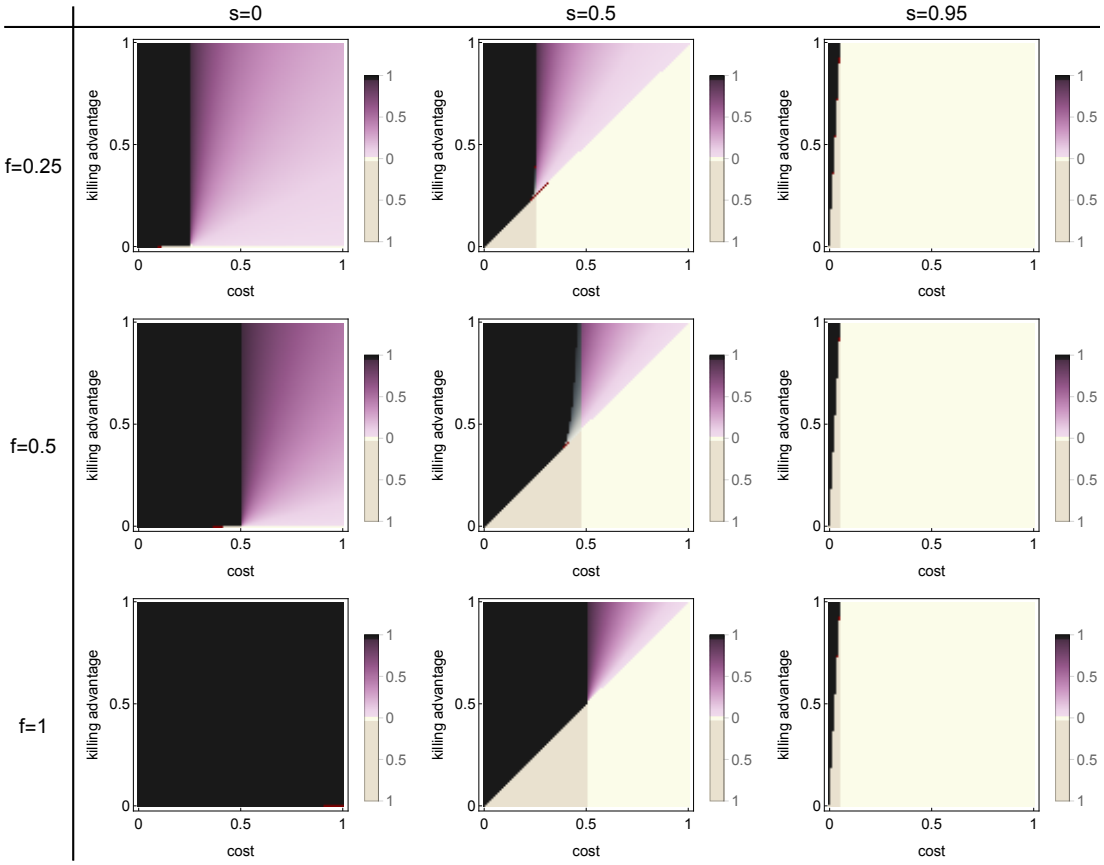

Figure S9: **Monokaryons in 1% of asci ($m = 0.01$) and recessive diploid fitness cost ($h_z = 0$). Equilibrium values and stability of the spore killer in *Podospora*, as a function of fitness cost, selfing rate (s), rate of first-division segregation (f) and killing advantage.** This figure can be compared to Figure S2 to see the effect of monokaryons in *Podospora*. Equilibrium values and stability were determined using deterministic simulations. Each graph gives equilibrium values for 100 values of fitness cost and 100 values of killing advantage.White cells correspond to $p_D = 0$ being a stable equilibrium and $p_D = 1$ being the only other (unstable) equilibrium. In these cases the spore killer cannot invade. Black cells correspond to $p_D = 1$ being a stable equilibrium with $p_D = 0$ being the only other (unstable) equilibrium, which means that the spore killer can invade and goes to fixation. Shades of purple indicate a stable internal equilibrium, which value is indicated by the scale next to each plot, with both $p_D = 0$ and $p_D = 1$ unstable. In that case, the spore killer can invade but will not reach fixation, a stable polymorphism can exist. Finally, beige areas represent an unstable internal equilibrium, which exact value cannot be determined by simulations. In that last case, both $p_D = 0$ and $p_D = 1$ are stable, meaning that the spore killer shouldn't be able to invade, but if present in the population at a frequency higher than the unstable equilibrium, it can then reach fixation. The grey area represents a space where two internal equilibria exist, one stable and one unstable, with the shading intensity representing the value of the stable one. The unstable equilibrium is always higher than the stable one so this area represents a parameter space where invasion is possible.

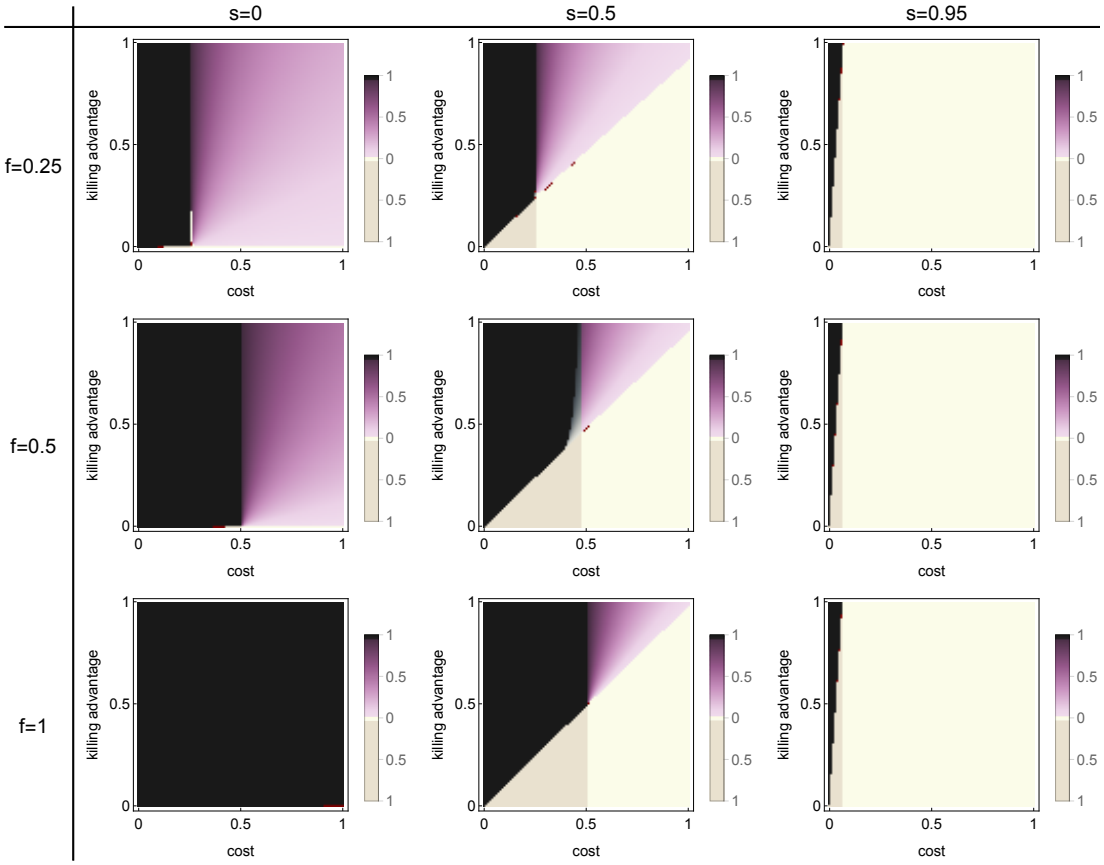

Figure S10: **Monokaryons in 5% of asci ($m = 0.05$) and recessive diploid fitness cost ($h_z = 0$). Equilibrium values and stability of the spore killer in *Podospora*, as a function of fitness cost, selfing rate (s), rate of first-division segregation (f) and killing advantage.** This figure can be compared to Figure S2 to see the effect of monokaryons in *Podospora*. Equilibrium values and stability were determined using deterministic simulations. Each graph gives equilibrium values for 100 values of fitness cost and 100 values of killing advantage.White cells correspond to $p_D = 0$ being a stable equilibrium and $p_D = 1$ being the only other (unstable) equilibrium. In these cases the spore killer cannot invade. Black cells correspond to $p_D = 1$ being a stable equilibrium with $p_D = 0$ being the only other (unstable) equilibrium, which means that the spore killer can invade and goes to fixation. Shades of purple indicate a stable internal equilibrium, which value is indicated by the scale next to each plot, with both $p_D = 0$ and $p_D = 1$ unstable. In that case, the spore killer can invade but will not reach fixation, a stable polymorphism can exist. Finally, beige areas represent an unstable internal equilibrium, which exact value cannot be determined by simulations. In that last case, both $p_D = 0$ and $p_D = 1$ are stable, meaning that the spore killer shouldn't be able to invade, but if present in the population at a frequency higher than the unstable equilibrium, it can then reach fixation. The grey area represents a space where two internal equilibria exist, one stable and one unstable, with the shading intensity representing the value of the stable one. The unstable equilibrium is always higher than the stable one so this area represents a parameter space where invasion is possible.

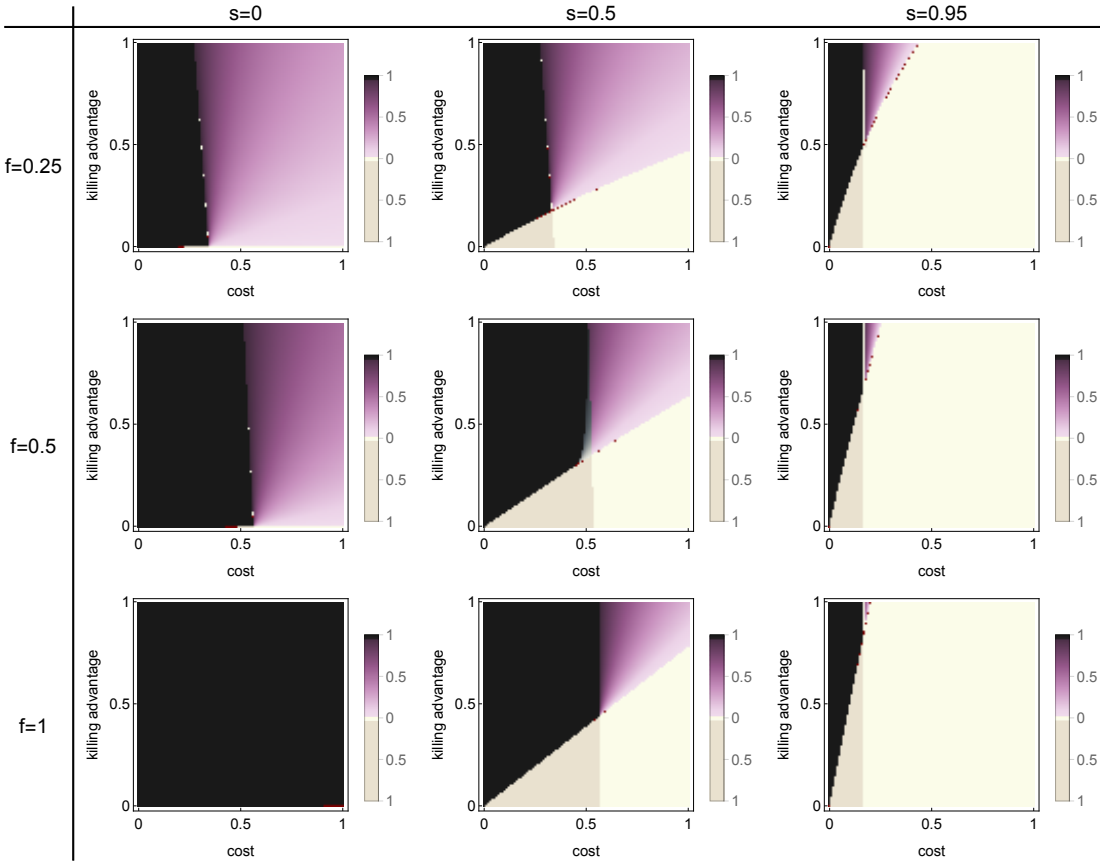

Figure S11: **Monokaryons in 50% of asci ($m = 0.50$) and recessive diploid fitness cost ($h_z = 0$). Equilibrium values and stability of the spore killer in *Podospora*, as a function of fitness cost, selfing rate (s), rate of first-division segregation (f) and killing advantage.** This figure can be compared to Figure S2 to see the effect of monokaryons in *Podospora*. Equilibrium values and stability were determined using deterministic simulations. Each graph gives equilibrium values for 100 values of fitness cost and 100 values of killing advantage.White cells correspond to $p_D = 0$ being a stable equilibrium and $p_D = 1$ being the only other (unstable) equilibrium. In these cases the spore killer cannot invade. Black cells correspond to $p_D = 1$ being a stable equilibrium with $p_D = 0$ being the only other (unstable) equilibrium, which means that the spore killer can invade and goes to fixation. Shades of purple indicate a stable internal equilibrium, which value is indicated by the scale next to each plot, with both $p_D = 0$ and $p_D = 1$ unstable. In that case, the spore killer can invade but will not reach fixation, a stable polymorphism can exist. Finally, beige areas represent an unstable internal equilibrium, which exact value cannot be determined by simulations. In that last case, both $p_D = 0$ and $p_D = 1$ are stable, meaning that the spore killer shouldn't be able to invade, but if present in the population at a frequency higher than the unstable equilibrium, it can then reach fixation. The grey area represents a space where two internal equilibria exist, one stable and one unstable, with the shading intensity representing the value of the stable one. The unstable equilibrium is always higher than the stable one so this area represents a parameter space where invasion is possible.

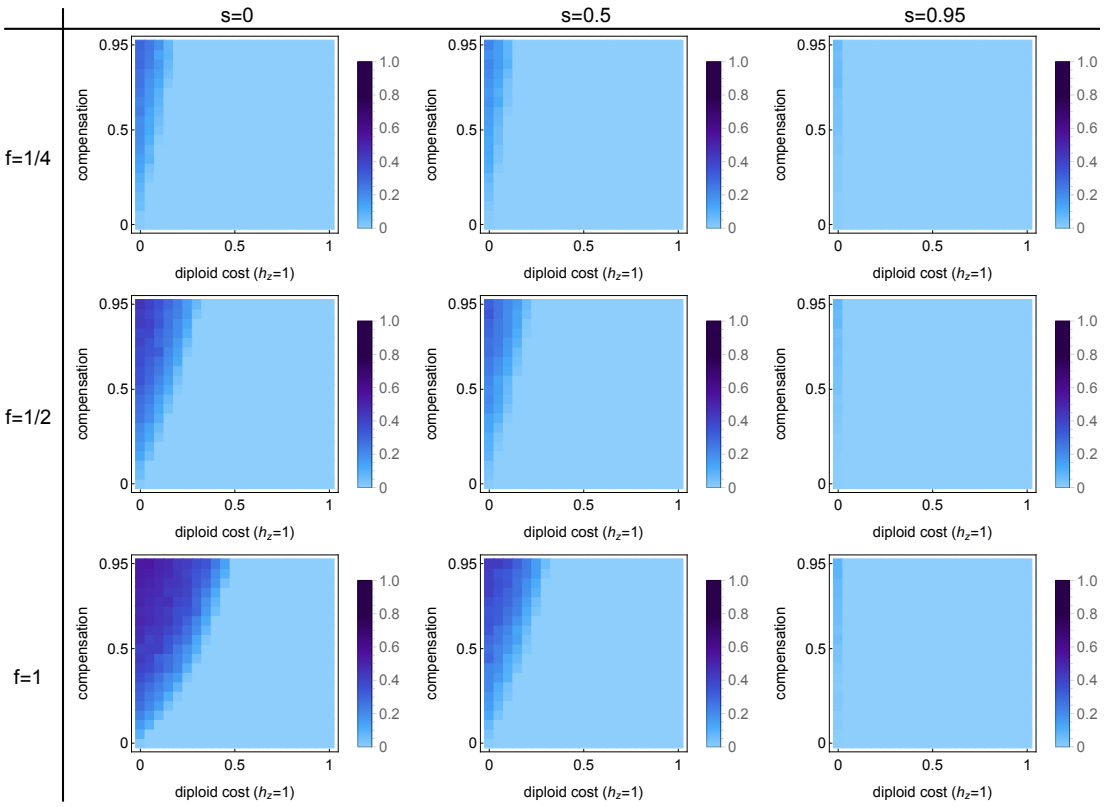

Figure S12: **Invasion probability of a spore killer with dominant diploid fitness cost ($h_z = 1$) in *Podospora* as a function of selfing rate (s), probability of first-division segregation (f) and killing advantage.** Each heatmap presents invasion probability of a spore killer allele as a function of fitness cost of carrying the allele (x-axis) and killing advantage a (y-axis). For each pixel, invasion probability is estimated from 10^3 stochastic simulations. Heatmaps are given for three values of selfing rate and three values of first-division segregation probability. The population size is 1000.

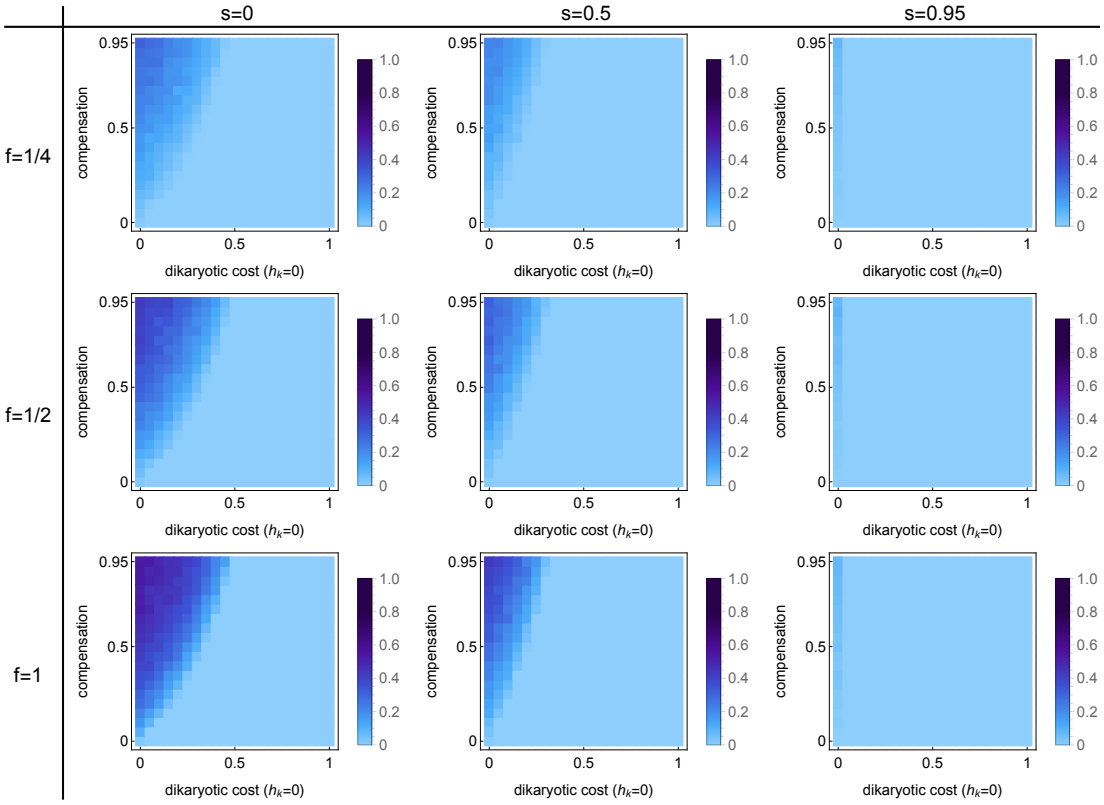

Figure S13: **Invasion probability of a spore killer with recessive dikaryotic fitness cost ($h_k = 0$) in *Podospora* as a function of selfing rate (s), probability of first-division segregation (f) and killing advantage.** Each heatmap presents invasion probability of a spore killer allele as a function of fitness cost of carrying the allele (x-axis) and killing advantage a (y-axis). For each pixel, invasion probability is estimated from 10^3 stochastic simulations. Heatmaps are given for three values of selfing rate and three values of first-division segregation probability. The population size is 1000.

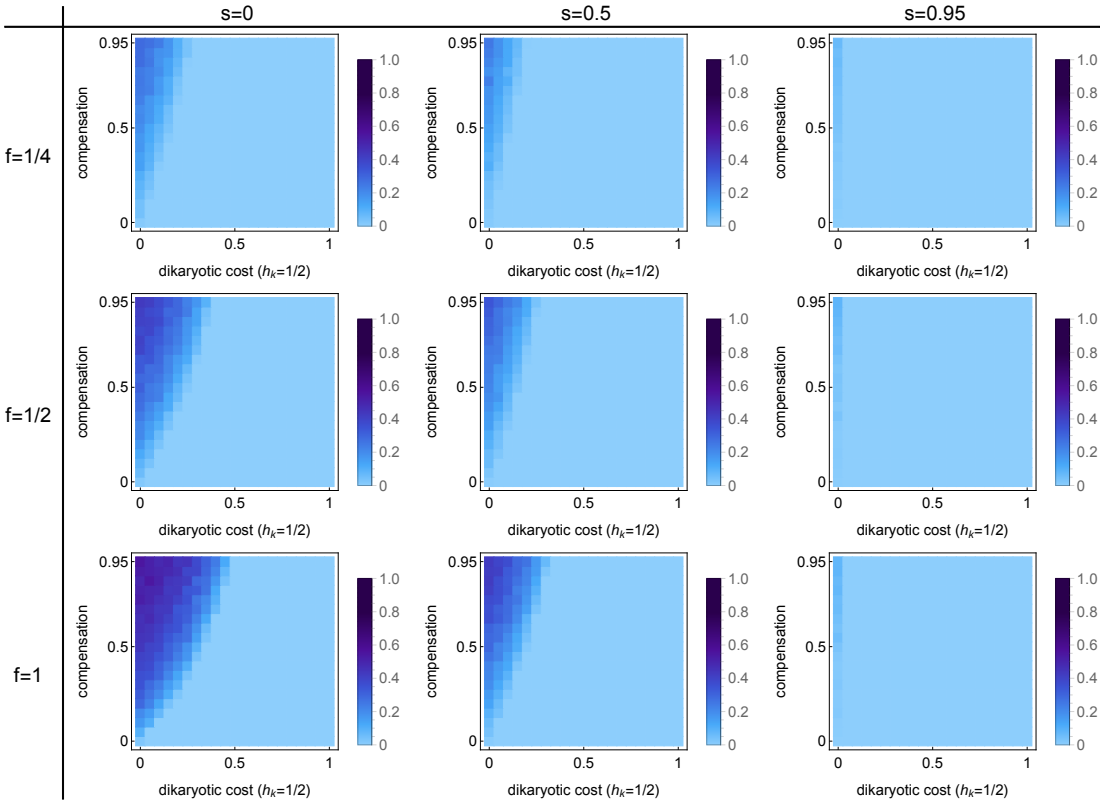

Figure S14: **Invasion probability of a spore killer with additive dikaryotic fitness cost ($h_k = 1/2$) in *Podospora* as a function of selfing rate (s), probability of first-division segregation (f) and killing advantage.** Each heatmap presents invasion probability of a spore killer allele as a function of fitness cost of carrying the allele (x-axis) and killing advantage a (y-axis). For each pixel, invasion probability is estimated from 10^3 stochastic simulations. Heatmaps are given for three values of selfing rate and three values of first-division segregation probability. The population size is 1000.

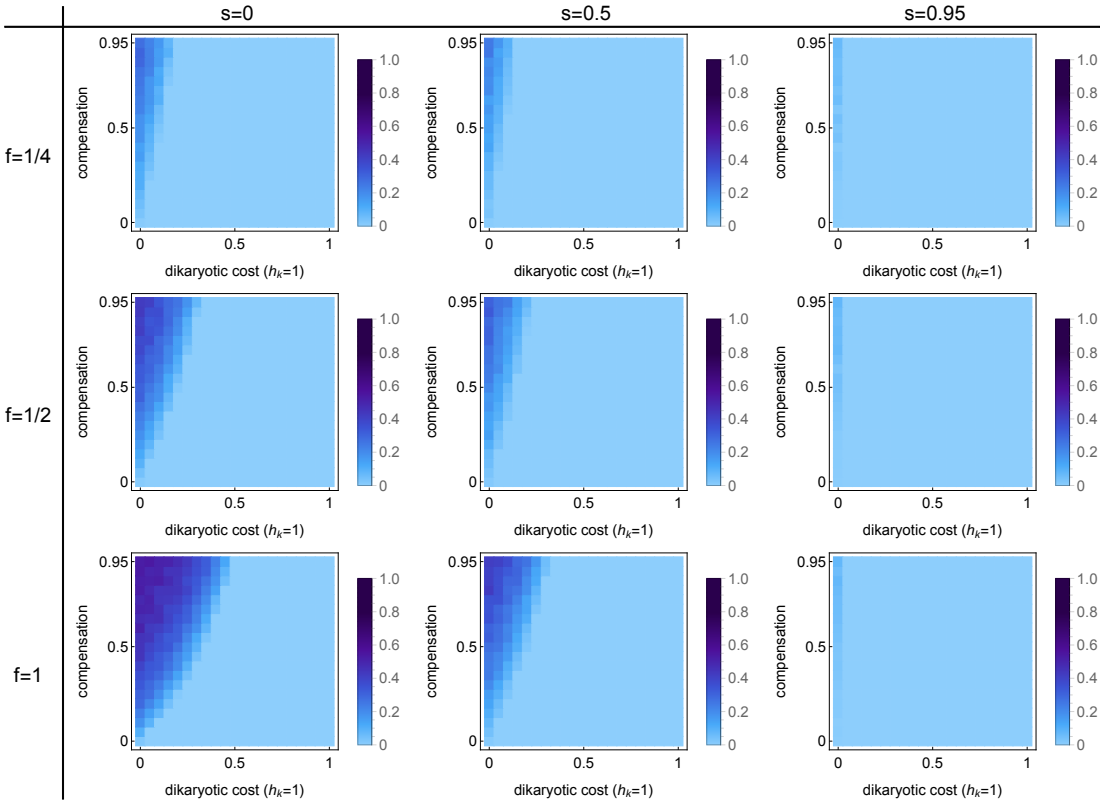

Figure S15: **Invasion probability of a spore killer with dominant dikaryotic fitness cost ($h_k = 1$) in *Podospora* as a function of selfing rate (s), probability of first-division segregation (f) and killing advantage.** Each heatmap presents invasion probability of a spore killer allele as a function of fitness cost of carrying the allele (x-axis) and killing advantage a (y-axis). For each pixel, invasion probability is estimated from 10^3 stochastic simulations. Heatmaps are given for three values of selfing rate and three values of first-division segregation probability. The population size is 1000.

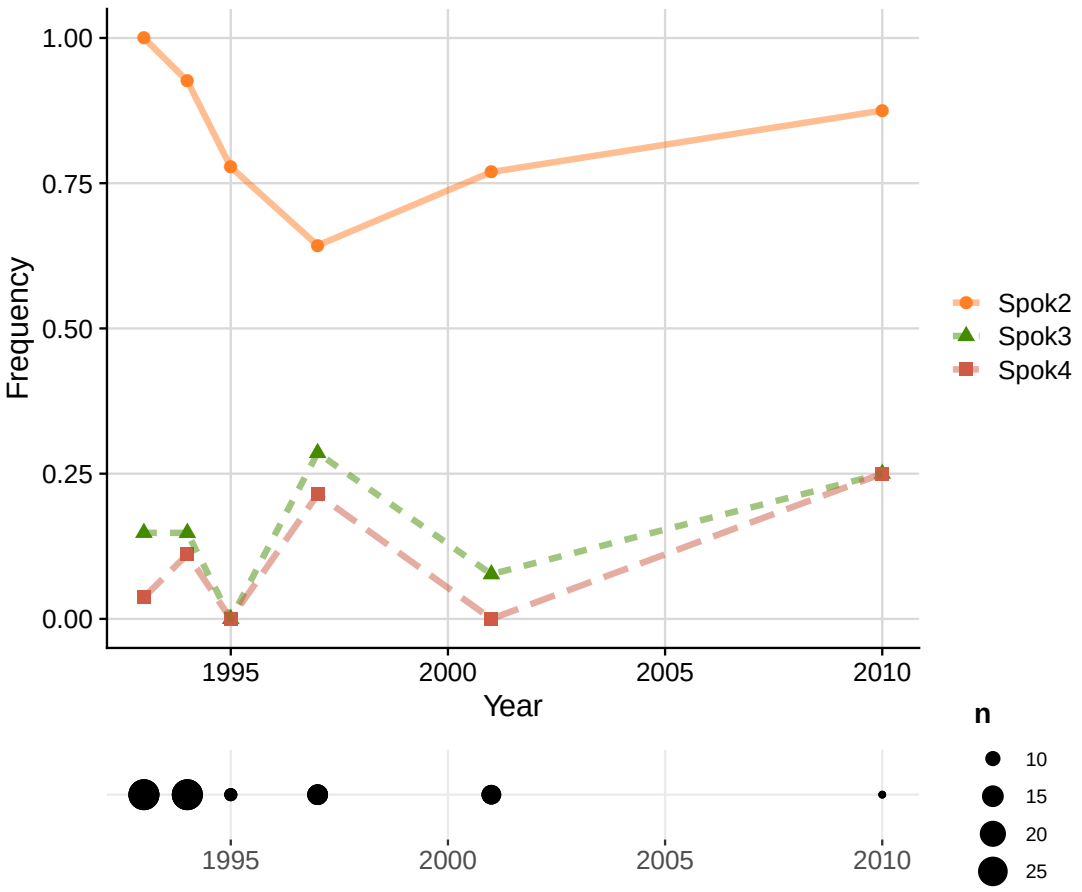

Figure S16: **Frequency of *Spok2*, *Spok3* and *Spok4* in the Wageningen population of *Podospora anserina* from 1993 to 2010**. Strains of *P. anserina* have been collected around Wageningen, the Netherlands, since the early 90s (van der Gaag, 2005). We used phenotypic, as well as published and unpublished genomic data to determine the *Spok* content of each strain, following (Vogan et al., 2019). n: sample size per year.

Appendix 1: Comparing absolute and relative meiotic drive

Purpose

To illustrate the qualitative differences in selective advantage between absolute and relative meiotic drive, we built a simple population genetics model somewhat similar to the one presented by Crow (1991). The novelty in our model is the possibility to vary the degree of compensation, or, in other words, the proportion of meiotic products suppressed by the action of the meiotic driver (MD) that get replaced by meiotic products carrying the MD. For example, in a female drive system all suppressed meiotic products are replaced by products carrying the MD (full compensation). In a male drive system, it is possible that some or all of the suppressed sperm cells are replaced (partial compensation). Finally, in a spore killing system, it has been proposed that suppressed meiotic products are not replaced (no compensation resulting in pure relative drive). This simple model aims to make clear the influence of the level of compensation on the dynamics of MDs. Since we are only interested in the effect of different levels of compensation, we assume no fitness difference between the different genotypes. Only suppression of meiotic products from heterozygotes and compensation influence the dynamics of the different alleles.

The model

We consider a one-locus drive system with two alleles, the driving allele D and the sensitive allele d. We consider an organism reproducing through random mating. The frequency of the driving allele is termed p_D and consequently the frequency of the sensitive equals $1 - p_D$. The action of meiotic drive is partitioned into two steps. First, the MD is able to suppress a proportion e ($0 \leq e \leq 1$) of the meiotic products. Then, a fraction c ($0 \leq c \leq e$) of the suppressed meiotic products can be replaced (compensation) by D carrying products. The model can be summarized by the change of allele frequencies during meiosis, which is compiled in Table A1.

Using the information from Table A1, the change in frequency of the driving allele D over one generation can be written as

$$p'_D = \frac{p_D^2 + p_D(1 - p_D)(1 + c)}{1 - (e - c)p_D(1 - p_D)}, \tag{A1}$$

where p'_D is the frequency of D at the next generation. We can define the selective advantage s of the drive as

$$1 + s = \frac{p'_D}{p_D}$$

so that a positive s means that D will increase in frequency. In our case, the selective advantage

Genotype (2N)	Frequency		Genotype (N)	Frequency
DD	p_D^2	$\longmapsto$	D	$p_D^2/\bar{w}$
Dd	$2p_D(1-p_D)$	$\nearrow$	D	$2p_D(1-p_D) \times \frac{1+c}{2}$
		$\searrow$	d	$2p_D(1-p_D) \times \frac{1-e}{2}$
dd	$(1-p_D)^2$	$\longmapsto$	d	$(1-p_D)^2$

Table A1: **Table of genotype frequencies before and after meiosis.** p_D is the frequency of the D allele before meiosis, e the efficiency of the drive at removing the alternative allele, and c the propensity of the driving allele at replacing suppressed meiotic products. $\bar{w}$ represents mean fitness, and is equal to the sum of the numerators of the entries in the last column of the table.

s of the driving allele is

$$s = \frac{1 + c(1-p_D)}{1-(e-c)p_D(1-p_D)} - 1. \tag{A2}$$

The following observations can be made. First, for $e > c$ and $p_D < 1$ we find $s > 0$. Thus, in a deterministic model the killing allele increases in frequency whenever the killing efficiency exceeds compensation. This holds in particular for the case of no compensation ($c = 0$). Second, for $p_D = 0$ we find $s = c$. Thus, for the case of female drive (equivalent to full compensation, $c = 1$) we find a maximal value of $s = 1$, while for male drive with no compensation we find $s = 0$. A more detailed analysis of the effect of drive efficiency e and the degree of compensation c is presented in Box 1 in the main manuscript.

Appendix 2: Invasion probability of a simple spore killer

Purpose

The calculations below are adapted from Desai and Fisher (2007), and give an approximation for the invasion probability of a spore killer with 100% killing efficiency but no killing advantage in a randomly-mating population (i.e., no selfing), starting from a single copy. The spore killer is said to have 'invaded' when it has reached a sufficient copy number that its dynamics are determined predominantly by the deterministic selective advantage it obtains from killing, rather than by random drift.

Heuristic calculation

As before, let p_D denote the frequency of the spore killer, which we assume to be small ($p_D \approx 0$). Setting $c = 0$ and $e = 1$ in Eq. (A2), we find that the selective advantage of the spore killer is

$$s = \frac{p_D(1 - p_D)}{1 - p_D(1 - p_D)} \approx p_D. \tag{A3}$$

Let n denote the absolute number of copies of the spore killer (so that $p_D = n/N$). Across each of the next n generations, the spore killer is expected to increase by approximately $ns = np_D = n^2/N$ copies (indeed, slightly more because the selective advantage comes to exceed $s = p_D$ as the spore killer increases in copy number), for a total expected gain of n^3/N copies. Meanwhile, over the same period, the standard deviation of the swing in copy number due to random drift is $\sim n$ (Desai and Fisher, 2007). Therefore, the deterministic force pushing the spore killer up in copy number dominates the random force that could push it down in copy number when $n^3/N > n$, i.e., when $n > \sqrt{N}$. Thus, the spore killer can be said to have invaded when it has attained $\sqrt{N}$ copies. Because its dynamics before this point are dominated by drift, the probability that it attains $\sqrt{N}$ copies having started as a single copy is approximately $\sqrt{N}/N = 1/\sqrt{N}$. As shown in Box 2 (figure panel a), this approximation accords well with estimates obtained from simulations of the model.

Comparison to a recessive beneficial allele

Consider a recessive beneficial allele D with selection coefficient 1. From a frequency of p_D, its change in frequency across one generation is

$$p'_D = \frac{p_D^2 \times 2 + 2p_D(1-p_D) \times 1 \times \frac{1}{2}}{1+p_D^2} = \frac{p_D(1+p_D)}{1+p_D^2}, \tag{A4}$$

so that the allele's selective advantage

$$s = \frac{p'_D}{p_D} - 1 = \frac{p_D(1-p_D)}{1+p_D^2}. \tag{A5}$$

When $p_D \ll 1$ (the relevant case for invasion),

$$s \approx p_D, \tag{A6}$$

as for the spore killer considered above [Eq. (A3)]. Thus, although they are not identical, the selective advantages of the spore killer and the recessive beneficial allele with selection coefficient 1 are similar when the two alleles are rare. This explains why the approximate invasion probability derived above for the spore killer resembles the fixation probability for a recessive beneficial mutation with selection coefficient 1 (Kimura, 1962, Eq. 15). It also explains why our result concerning the invasion rate of spore killers in a subdivided population, derived in Box 2, matches the analogous result for recessive beneficial mutations (Gale, 1990, p. 180-181).